

9437

NACA TN 3141

0065968



TECH LIBRARY KAFB, NM

NATIONAL ADVISORY COMMITTEE FOR AERONAUTICS

TECHNICAL NOTE 3141

COMBINED NATURAL- AND FORCED-CONVECTION LAMINAR FLOW
AND HEAT TRANSFER OF FLUIDS WITH AND WITHOUT
HEAT SOURCES IN CHANNELS WITH LINEARLY
VARYING WALL TEMPERATURES

By Simon Ostrach

Lewis Flight Propulsion Laboratory
Cleveland, Ohio



Washington

April 1954

AFMDC
TECHNICAL LIBRARY
APR 20 1954



 TECHNICAL NOTE 3141

 COMBINED NATURAL- AND FORCED-CONVECTION LAMINAR FLOW AND
 HEAT TRANSFER OF FLUIDS WITH AND WITHOUT HEAT SOURCES IN
 CHANNELS WITH LINEARLY VARYING WALL TEMPERATURES

By Simon Ostrach

SUMMARY

The flow of fluids with and without heat sources and subject to body forces between two plane parallel surfaces which are oriented in the direction of the generating body force is analyzed under the condition that the temperature vary linearly along these surfaces. It is found that a modified Rayleigh number (product of the reciprocal of the ratio of specific heats and the Prandtl number Pr and the modified Grashof number Gr_A) as well as a parameter $K_A = Pr Gr_A \frac{\beta f_X d}{c_p}$ is of significance in this problem; where β is the volumetric expansion coefficient, f_X is the negative of the X-component of body force per unit mass, d is the characteristic length, and c_p is the specific heat at constant pressure. Solutions of this problem are obtained in terms of "universal" functions which are tabulated for simple application to specific cases. Representative velocity and temperature distributions from which detailed study of the heat transfer is made are then computed. When the ratio of CK_A (where C is related to the mass flow) to the Rayleigh number is of unit order of magnitude, the effects of aerodynamic or frictional heating can be appreciable. Asymptotic solutions (for large values of the Rayleigh number) which render the computations simple are also presented.

Comparison of the results from the method given herein with those obtained elsewhere in an approximate manner for a special case simulating the natural-convection flow of fluids with heat sources in a completely enclosed region shows that the approximate method is sufficiently accurate for problems in which the modified Rayleigh number is less than 10^4 .

INTRODUCTION

In recent years the transfer of heat to and from enclosed or partially enclosed regions by means of natural convection or by a combination of natural and forced convection has taken on new significance in the fields of aeronautics, atomic power, electronics, and chemical engineering. Most of the information on these modes of heat transfer under such conditions is of a semiempirical or specialized nature; relatively little detailed information exists for internal natural-convection flows. In reference 1 there appears one of the few attempts to determine theoretically the velocity and temperature distributions in detail and hence the heat transfer for an internal flow problem of this kind. In that reference a solution was found for the fully developed flow of fluids with and without heat sources between two long parallel plates with constant wall temperatures (where one could be different from the other) oriented in the direction of the generating body force. The information obtained therein is of practical value in connection with fully developed flows subject to body forces where the surfaces are maintained at uniform temperatures. Lighthill (ref. 2) employs integral methods to study the natural-convection flow in tubes with either one end or both ends closed and with constant wall temperatures, and in reference 3 approximate superimposed free- and forced-convection flows are obtained for short channels and pipes.

As the next step in the study of natural convection or combined natural and forced flows in confined spaces, consideration is here given to the configuration of reference 1 with the exception that the thermal boundary condition specified is that the surface temperatures vary linearly along the plates or surfaces. (One surface, however, may be at a different local temperature from the other but the slopes of the temperature distributions on each surface are taken to be equal.) The analogous forced-convection problem is treated in references 4, 5, and 6. The present problem simulates several important physical occurrences of this phenomenon; for example, it could represent the case where the outside of the channel formed by the plates is cooled (or heated) by a counterflow. In addition, the present problem represents a more general case than was considered in reference 1, since here the temperature will no longer be restricted to be a function of the transverse coordinate alone and, hence, energy convective as well as mass convective effects will be included.

The solution is obtained in terms of functions which depend on only one of the several associated dimensionless parameters, and these functions are tabulated so that specific cases can be easily computed. Solutions for pure natural convection and for superimposed natural and forced convection are shown to be essentially identical. Representative velocity and temperature distributions are also presented, and the effects of frictional or aerodynamic heating on the flow and heat transfer are discussed.

A special case which simulates a completely enclosed region in which there is no net mass flow, the walls are at the same temperature, and heat is generated uniformly by heat sources is treated, and detailed velocity and temperature profiles are obtained from which the heat transfer is determined. This special case was treated in an approximate manner in reference 7.

Consideration is also given to the problem of convective inversion, that is, to the cases where the modified Grashof number changes sign. It is shown that convective inversion due to changes in the body force direction, to changes in the sign of the volumetric expansion coefficient, or to changes in the sign of the axial temperature gradient alters the character of the problem, because, it is believed, under these conditions the flow becomes unstable because of heating from below (see pp. 104 to 107, ref. 8).

ANALYSIS

Formulation of the Problem

The study to be made here is that of the laminar fully developed flow of fluids with and without heat sources and subject to a body force between two plane parallel surfaces open at both ends and oriented in the direction of the generating body force (see fig. 1). It is further specified that there shall be linear (with equal slopes) temperature variations along the walls but that the walls need not necessarily be at the same temperature. The flow is assumed to be parallel to the axis of the channel (that is, the only nonvanishing velocity component is the one in the longitudinal direction) and in addition it is assumed that the physical properties (for example, c_p and μ) of the fluids are constants and that the essential influence of the density changes on the flow is taken into account by the introduction of the volumetric expansion coefficient in the body force term (that is, the other influences of variable density and the variation of the expansion coefficient with temperature are negligible). Discussions of the justification of the assumptions can be found in references 1, 9, and 10.

Under the conditions stated, the basic equations with body forces included expressing the conservation of mass, momentum, and energy (see ref. 1) become, respectively,

$$\frac{\partial U}{\partial X} = 0 \quad (1)$$

$$\frac{\partial^2 U}{\partial Y^2} = \frac{1}{\mu} \left(\rho f_X + \frac{\partial P}{\partial X} \right) \quad (2)$$

$$\frac{\partial P}{\partial Y} = 0 \quad (3)$$

$$\frac{\partial^2 T^*}{\partial X^2} + \frac{\partial^2 T^*}{\partial Y^2} = \frac{\rho c_v}{k} U \frac{\partial T^*}{\partial X} - \frac{\mu}{k} \left(\frac{\partial U}{\partial Y} \right)^2 - \frac{Q}{k} \quad (4)$$

(See appendix A for a complete list of the symbols used herein.) With cognizance taken of equations (1) and (3) the above system reduces to

$$\frac{d^2 U}{dY^2} = \frac{1}{\mu} \left(\rho f_X + \frac{dP}{dX} \right) \quad (5)$$

$$\frac{\partial^2 T^*}{\partial X^2} + \frac{\partial^2 T^*}{\partial Y^2} = \frac{\rho c_v}{k} U \frac{\partial T^*}{\partial X} - \frac{\mu}{k} \left(\frac{\partial U}{\partial Y} \right)^2 - \frac{Q}{k} \quad (6)$$

where the velocity is a function of the transverse coordinate Y only and the pressure is a function of only the longitudinal coordinate.

The body force term in equation (5) can be written as a buoyancy term by introducing the volumetric expansion coefficient β in a manner similar to that described in appendix B of reference 1. Equation (5) then becomes

$$\frac{d^2 U}{dY^2} + \frac{\rho \beta f_X}{\mu} (T^* - T_{w0}^*) = \frac{1}{\mu} \left(\frac{dP}{dX} + \rho_{w0} f_X \right) \quad (7)$$

where the subscript w_0 refers to the surface at $Y = 0$ (see fig. 1).

The boundary conditions associated with this problem are that the velocity at the walls must vanish (the no-slip condition for viscous fluids) and that the temperature must vary linearly along the walls. (Note that the latter condition implies that the temperature gradients along the walls and hence the axial heat flux along the walls must be constant.) In order to satisfy the temperature conditions and equation (7), the temperature must be of the form

$$T^*(X, Y) = AX + T(Y) \quad (8)$$

Mathematically, the boundary conditions are formulated as

$$U(0) = U(d) = 0 \quad (9)$$

$$T^*(X, 0) = AX + T(0) \quad (10)$$

$$T^*(X, d) = AX + T(d) \quad (11)$$

Substituting equation (8) into equations (7) and (6), respectively, yields

$$\frac{d^2U}{dY^2} + \frac{\rho\beta f_X}{\mu} \theta = \frac{1}{\mu} \left(\frac{dP}{dX} + \rho_{w0} f_X \right) \quad (12)$$

and

$$\frac{d^2\theta}{dY^2} - \frac{\rho c_v A}{k} U + \frac{\mu}{k} \left(\frac{dU}{dY} \right)^2 + \frac{Q}{k} = 0 \quad (13)$$

where

$$\theta = T(Y) - T(0)$$

Since the left side of equation (12) is a function of Y alone and the right side is a function of X alone, it is clear that each side must be equal to a constant. Thus, equation (12) can be written as

$$\frac{d^2U}{dY^2} + \frac{\rho\beta f_X}{\mu} \theta = \bar{C} \quad (14a)$$

or

$$\frac{1}{\mu} \left(\frac{dP}{dX} + \rho_{w0} f_X \right) = \bar{C} \quad (14b)$$

The temperature now appears in equations (13) and (14) as θ which is independent of the longitudinal coordinate X , and hence the thermal boundary conditions can be written as

$$\begin{aligned} \theta(0) &= 0 \\ \theta(d) &= T(d) - T(0) \equiv \theta_{w1} \end{aligned} \quad (15)$$

To nondimensionalize equations (14) and (13), let

$$\left. \begin{aligned} U &= \frac{ku}{\rho \beta f_X d^2} = u \sqrt{\frac{c_p Ad}{Pr K_A}} \\ Y &= yd \\ \theta &= \frac{\mu k \tau}{\rho^2 \beta^2 f_X^2 d^4} = \frac{Ad}{K_A} \tau \end{aligned} \right\} \quad (16)$$

where $K_A = Pr Gr_A \left(\frac{\beta f_X d}{c_p} \right)$ is the new dimensionless parameter presented

in reference 1, but here the Grashof number is modified because it is based on Ad rather than on a temperature difference, that is,

$Gr_A = \frac{\beta f_X d^4 A}{\nu^2}$. Hence, equations (14), (13), (9), and (15) become

$$u'' + \tau = CK_A \quad (17)$$

$$\tau'' - Ra u + (u')^2 + \alpha K_A = 0 \quad (18)$$

$$u(0) = u(1) = 0 \quad (19)$$

$$\tau(0) = 0 \quad (20)$$

$$\tau(1) = \frac{K_A \theta_{w1}}{Ad} \quad (21)$$

where the primes denote differentiation with respect to y , $Ra = (1/\gamma) Pr Gr_A$ is a modified Rayleigh criterion or number (see p. 105, ref. 8), $\alpha = Qd/kA$ is the dimensionless heat source parameter, and $C = \bar{C} \sqrt{Pr d^3 / c_p A K_A}$. Eliminating τ between equations (17) and (18) results in

$$u^{iv} - (u')^2 + Ra u - \alpha K_A = 0 \quad (22)$$

with the boundary conditions

$$u(0) = u(1) = 0 \quad (23)$$

$$u''(0) = CK_A \quad (24)$$

$$u''(1) = (C - \theta_{w1}/Ad) K_A = mCK_A \quad (25)$$

where $m = 1 - \theta_w/CAd$. The constant C which appears as a parameter in the boundary-value problem described by equations (22) to (25) merely specifies the temperature level (see eq. (17)) of the problem. In order to define completely the temperatures and velocities, this constant must be related in some way to the physics of the problem. From equation (14b) it can be seen that C could be determined from the pressure gradient along the channel; that is, C is essentially connected with the end conditions to which the channel is subject. Since the pressure gradient may not be known a priori, in the subsequent section dealing with the solution of the present problem C will be related to the end conditions by the mass flow in the channel, which remains invariant over the entire length of the channel.

Note that solution of the preceding boundary-value problem will yield velocity and temperature distributions for both natural-convection and combined natural- and forced-convection flows. The forced-convection pressure gradient merely alters the magnitude of the constant C . A discussion of such a superimposed flow problem under special conditions is given in reference 11.

Several interesting observations can now be made concerning these equations. First, comparison of equation (22) with the corresponding equation in reference 1 shows that they are identical except for the third term in equation (22), which does not appear at all in the equation in reference 1. This term stems from the convection term in the energy equation; hence, in the present problem energy convection effects will be included. The energy convection term vanished identically in reference 1 because of the assumption that the velocity and temperature profiles were independent of the axial coordinate. Second, since the convection term appears with a coefficient, another dimensionless parameter (Ra , the modified Rayleigh number) is associated with this problem and its influence on the results must be studied. Finally, the conditions of the problem require that the temperature be of the form $T^* = AX + T(y)$ (see eq. (8)), and hence the longitudinal heat flux is everywhere constant.

The boundary-value problem stated in equations (22) to (25) can be written in more convenient form by defining

$$\bar{v} = Ra \, u - \alpha K_A \quad (26)$$

Hence

$$\frac{dv}{dy} + Ra \, \bar{v} - \frac{1}{Ra} (\bar{v}')^2 = 0 \quad (27)$$

$$\bar{v}(0) = \bar{v}(1) = -\alpha K_A \quad (28)$$

$$\bar{v}''(0) = +Ra \, CK_A \quad \bar{v}''(1) = +m \, Ra \, CK_A \quad (29)$$

Solutions of the Boundary-Value Problem

Equation (27) is nonlinear (the nonlinear term is due to the frictional or aerodynamic heating) and therefore, as in reference 1, a method of successive approximations will be employed to find its solution. To this end, equation (27) is written

$$\frac{dv}{dy} + Ra \, \bar{v}_n - \frac{1}{Ra} (\bar{v}'_{n-1})^2 = 0 \quad (30)$$

where $n = 0, 1$ denotes the particular term in the approximation $v = v_0 + v_1$ and $v'_{-1} \equiv 0$. Let

$$\left. \begin{aligned} v &= \frac{1}{64} \bar{v} \\ \eta &= 2y - 1 \\ \lambda &= -\frac{\alpha K_A}{64} \\ J &= \frac{Ra^{1/2} CK_A}{64} \\ R &= \frac{Ra}{16} \end{aligned} \right\} \quad (31)$$

Equations (30), (28), and (29) become, respectively,

$$v_n^{iv} + Rv_n - \frac{1}{R}(v_{n-1}')^2 = 0 \quad (32)$$

$$v_0(-1) = v_0(1) = \lambda \quad (33)$$

$$v_0''(-1) = J\sqrt{R} \quad v_0''(1) = mJ\sqrt{R} \quad (34a)$$

$$v_n(-1) = v_n(1) = v_n''(-1) = v_n''(1) = 0 \quad n \neq 0 \quad (34b)$$

where the subscripts now denote differentiation with respect to η .

Zeroth-order approximation. - In the zeroth-order approximation, the nonlinear term which is associated with the frictional heating does not appear and the problem then consists of solving the equation

$$v_0^{iv} + Rv_0 = 0 \quad (35)$$

subject to the boundary conditions

$$v_0(-1) = v_0(1) = \lambda \quad (36)$$

$$v_0''(-1) = J\sqrt{R} \quad v_0''(1) = mJ\sqrt{R} \quad (37)$$

For simplicity of computations the solution can be obtained in terms of symmetric and antisymmetric functions of η , depending only on the parameter R (or Ra), by setting

$$v_0 = \lambda v_{00} + \frac{J(m-1)}{2} v_{01} + \frac{J(m+1)}{2} v_{02} \quad (38)$$

where the boundary conditions to be satisfied by the various v_{0j} (where $j = 0, 1, 2$) are given in the following table:

Subscript	$v(-1)$	$v(1)$	$v''(-1)$	$v''(1)$
00	1	1	0	0
01	0	0	$-\sqrt{R}$	\sqrt{R}
02	0	0	\sqrt{R}	\sqrt{R}

The functions v_{0j} must each satisfy equation (35), which has the general solution for positive values of the Rayleigh number

$$v_0 = a_1 \exp(er\eta) + a_2 \exp(-er\eta) + a_3 \exp(gr\eta) + a_4 \exp(-gr\eta) \quad (39)$$

where

$$e = 1 + i$$

$$g = 1 - i$$

and

$$r = R^{1/4}/\sqrt{2}$$

Using the boundary conditions to evaluate the constants in equation (39) and expressing the solution in terms of real products of circular and hyperbolic functions show that

$$\begin{aligned} v_{00} = \frac{1}{\cosh^2 r + \cos^2 r - 1} & (\cosh r \cos r \cosh r\eta \cos r\eta \\ & + \sinh r \sin r \sinh r\eta \sin r\eta) \end{aligned} \quad (40)$$

$$\begin{aligned} v_{01} = \frac{1}{\cos^2 r - \cosh^2 r} & (\cosh r \sin r \sinh r\eta \cos r\eta \\ & - \sinh r \cos r \cosh r\eta \sin r\eta) \end{aligned} \quad (41)$$

$$\begin{aligned} v_{02} = \frac{1}{\cosh^2 r + \cos^2 r - 1} & (\cosh r \cos r \sinh r\eta \sin r\eta \\ & - \sinh r \sin r \cosh r\eta \cos r\eta) \end{aligned} \quad (42)$$

Note that v_{00} and v_{02} are symmetric functions and v_{01} is an anti-symmetric function of η . These "universal" functions v_{0j} are given for various values of Ra in table I.

First-order approximation. - In order to include the effects of frictional heating to a first order, let $n = 1$ in equation (32). Thus

$$v_1^{iv} + Rv_1 = \frac{1}{R} (v_0')^2 = f(\eta) \quad (43)$$

where, in view of equation (38), $f(\eta)$ is given by

$$f(\eta) = \frac{1}{R} \left[\lambda^2 v_{00}'^2 + \lambda J(m+1) v_{00}' v_{02}' + \frac{J^2(m-1)^2}{4} v_{01}'^2 + \frac{J^2(m+1)^2}{4} v_{02}'^2 + \lambda J(m-1) v_{00}' v_{01}' + \frac{J^2(m^2-1)}{2} v_{01}' v_{02}' \right] \quad (44)$$

The boundary conditions on v_1 are

$$v_1(-1) = v_1(1) = v_1''(-1) = v_1''(1) = 0 \quad (45)$$

Once again, to obtain "universal-type" functions let

$$v_1 = \lambda^2 v_{10} + \lambda J(m+1) v_{11} + \frac{J^2(m-1)^2}{4} v_{12} + \frac{J^2(m+1)^2}{4} v_{13} + \lambda J(m-1) v_{14} + \frac{J^2(m^2-1)}{2} v_{15} \quad (46)$$

In view of the form of equations (43) to (46), the functions v_{10} , v_{11} , v_{12} , and v_{13} are symmetric; and v_{14} and v_{15} are antisymmetric functions. Each of the functions v_{1k} ($k = 0, 1, \dots, 5$) will be a solution of equation (43), but where the nonhomogeneous term is only the related part of equation (44) (for example, the first term on the right-hand side of equation (44) is associated with the v_{10} solution and so forth).

A particular solution of equation (43) can be constructed from

$$(v_{1k})_P = \int_0^\eta f_k(\xi) G(\eta - \xi) d\xi$$

where G is the Green's function which satisfies the homogeneous part of equation (43) and the conditions $G(0) = G'(0) = G''(0) = 0$, $G'''(0) = 1$. These arbitrary conditions were applied to yield a simple form for the Green's function. Hence

$$(v_{1k})_P = -\frac{1}{8r^3} \int_0^\eta \left[e \sinh g r(\eta - \xi) - g \sinh e r(\eta - \xi) \right] f_k(\xi) d\xi \quad (47)$$

Note that if the f_k is a symmetric function, $(v_{1k})_P$ is also symmetric; and if f_k is antisymmetric, so is $(v_{1k})_P$. From the boundary conditions, equation (45), it can be seen that v_{1k} must be either symmetric or antisymmetric. Therefore, if f_k is symmetric, the complementary solution used with the particular solution must be symmetric; and if f_k is antisymmetric, the complementary solution must also be antisymmetric. These complementary solutions are, respectively,

$$(v_{1k})_{cs} = E \frac{\cosh er\eta}{\cosh er} + F \frac{\cosh gr\eta}{\cosh gr} \quad (48)$$

$$(v_{1k})_{ca} = E \frac{\sinh er\eta}{\sinh er} + F \frac{\sinh gr\eta}{\sinh gr} \quad (49)$$

$$E = \frac{e}{8r^3} \int_0^1 \left[\sinh er(1 - \xi) \right] f_k(\xi) d\xi \quad (50)$$

$$F = \frac{g}{8r^3} \int_0^1 \left[\sinh gr(1 - \xi) \right] f_k(\xi) d\xi \quad (51)$$

The v_{1k} solutions can be written explicitly in real form (by proper combinations of particular and complementary solutions) and are given in equations (B1) to (B6) in appendix B. Values of v_{1k} for several R (or Ra) are presented in table II.

Velocity and Temperature Distributions

Now that the various v_{1k} are known explicitly, they can be inserted into equation (46) to yield v_1 . The sum of v_0 (as given by eq. (38))

and v_1 then forms the solution which includes frictional heating effects to a first order. By means of the various transformations made, the solutions of the given boundary-value problem (eqs. (22) to (25)) or the dimensionless velocity distributions to the zeroth and first approximation are, respectively,

$$u_0 = \frac{K_A}{Ra} \left[-\alpha v_{00} + \frac{(m-1) Ra^{1/2} C}{2} v_{01} + \frac{(m+1) Ra^{1/2} C}{2} v_{02} + \alpha \right] \quad (52)$$

$$\begin{aligned} u_1 = \frac{1}{Ra} \left[64(v_0 + v_1) + \alpha K \right] = u_0 + \frac{K_A^2}{64 Ra} \left[\alpha^2 v_{10} - \alpha Ra^{1/2} C (m+1) v_{11} \right. \\ \left. + \frac{(m-1)^2 Ra C^2}{4} v_{12} + \frac{(m+1)^2 Ra C^2}{4} v_{13} - (m-1) \alpha Ra^{1/2} C v_{14} \right. \\ \left. + \frac{(m^2-1) Ra C^2}{2} v_{15} \right] \quad (53) \end{aligned}$$

where the v_{0j} ($j = 0, 1, 2$) are given in equations (40) to (42) and the v_{1k} ($k = 0, 1, 2, 3, 4, 5$) are given in appendix B.

In principle, higher-order approximations could be obtained by continuing the procedure described. However, the results become very unwieldy. Therefore, beyond the range of applicability of the zeroth- and first-order approximations (that is, in the range of large frictional heating effects), the complete boundary-value problem should be solved numerically; some discussion of these numerical results relative to the zeroth- and first-order approximations will be presented subsequently.

To determine the temperature distributions, recall that they are related to the velocity distributions by equation (17) and that

$$v''_{00} = -\frac{Ra^{1/2}}{4} v_{02} \quad \text{and} \quad v''_{02} = \frac{Ra^{1/2}}{4} v_{00} \quad \text{so that}$$

$$\tau_0 = CK_A - u''_0 = K_A \left\{ C - \frac{1}{Ra^{1/2}} \left[\alpha v_{02} + 2(m-1) C v''_{01} + \frac{(m+1)C}{2} Ra^{1/2} v_{00} \right] \right\} \quad (54)$$

and

$$\begin{aligned} \tau_1 = CK_A - u_1'' = \tau_0 - \frac{K_A^2}{16Ra} \left[\alpha^2 v_{10}'' - \alpha Ra^{1/2} C(m+1) v_{11}'' \right. \\ \left. + \frac{(m-1)^2 Ra C^2}{4} v_{12}'' + \frac{(m+1)^2 Ra C^2}{4} v_{13}'' - (m-1) \alpha Ra^{1/2} C v_{14}'' \right. \\ \left. + \frac{(m-1)^2 Ra C^2}{2} v_{15}'' \right] \end{aligned} \quad (55)$$

where the primes on the u-functions denote differentiations with respect to y and on the v-functions denote differentiations with respect to η , and the explicit forms of the second derivatives appearing in equations (54) and (55) are presented in equations (B7) to (B13) of appendix B.

Thus, solutions of the original boundary-value problem in terms of u and τ are known to zeroth- and first-order approximations, that is, neglecting frictional heating and including its effects to a first order, respectively. These solutions are, however, given in terms of the parameter C (recall that m is also a function of C through eq. (25)). Therefore, to relate C to the physical problem the dimensionless mass flow in the channel is defined as

$$M = \int_0^1 u_0 dy \quad (56)$$

Neglecting aerodynamic heating, equation (56) becomes (using the zeroth-order approximation as given by eq. (52))

$$\begin{aligned} M = \int_0^1 u_0 dy = \frac{K_A}{Ra} \left[\alpha - \frac{\sqrt{2} \alpha}{Ra^{1/4}} \left(\frac{\sin 2r + \sinh 2r}{\cosh 2r + \cos 2r} \right) \right. \\ \left. + Ra^{1/4} \frac{C(m+1)}{\sqrt{2}} \left(\frac{\sin 2r - \sinh 2r}{\cosh 2r + \cos 2r} \right) \right] \end{aligned} \quad (57)$$

or

$$C = \frac{\theta_{w1}}{2Ad} + \frac{1}{\sqrt{2} Ra^{1/4}} \left(\frac{\cosh 2r + \cos 2r}{\sin 2r - \sinh 2r} \right) \left[\frac{MRa}{K_A} - \alpha + \frac{\sqrt{2} \alpha}{Ra^{1/4}} \left(\frac{\sin 2r + \sinh 2r}{\cosh 2r + \cos 2r} \right) \right] \quad (58)$$

(For large Ra the expressions in parentheses in equation (58) reduce to 1 and -1, respectively.) Substitution of C as determined into equations (52) to (55) then yields the velocity and temperature distributions for any case if M , θ_{w1}/Ad , Ra , α , and K_A are known. Note, then, that the mass flow is an independent parameter of the problem, and hence could be due in part to a forced flow. For a given configuration and fluid the last four of these parameters are specified, so that equation (58) relates C to the mass flow M , that is, the temperature level and the mass flow through the channel are related, as is only reasonable in flows of this type.

Asymptotic solutions. - The solutions presented in the previous sections are valid (to the proper order of approximation) for all values of the parameters of the boundary-value problem. However, from physical considerations, it can be seen that in many practical occurrences of the phenomenon under consideration, the parameter Ra may become very large (of the order of 10^4 and higher). It is therefore appropriate to examine the asymptotic character of the boundary-value problem. To this end it is convenient to write equations (22) to (25) as

$$\frac{1}{Ra} \bar{u}^{iv} - \frac{K_A C}{Ra} (\bar{u}')^2 + \bar{u} - \frac{\alpha}{CRa} = 0 \quad (59)$$

$$\bar{u}(0) = \bar{u}(1) = 0 \quad (60)$$

$$\bar{u}''(0) = 1 \quad \bar{u}''(1) = m \quad (61)$$

where

$$u = CK_A \bar{u} \quad (62)$$

For very large Ra , equation (59) is of the boundary layer type (see ref. 10). Therefore the velocity and temperature profiles will have very large gradients near the walls, and thus the asymptotic solutions will yield the velocity and thermal boundary layers with essentially constant conditions given by the inviscid solution $\bar{u}_I = \alpha/CRa$ in the center of the channel associated with large Ra flows. Hence, expanding the coordinate normal to the wall, as is done in boundary layer theory, requires that

$$\bar{y} = Ra^{1/4} y \quad (63)$$

$$\bar{u} = Ra^{-1/2} v \quad (64)$$

The asymptotic forms of equations (59) to (61) are

$$V \frac{\partial^4 V}{\partial y^4} + V - \frac{CK_A}{Ra} (V_y)^2 - \frac{\alpha}{C Ra} \frac{1}{2} = 0 \quad (65)$$

$$V(0) = 0 \quad (66)$$

$$V_y(0) = \bar{m} = \begin{cases} 1 & \text{for the wall at temperature } T_{w0} \\ m & \text{for the other wall at temperature } T_{w1} \end{cases} \quad (67)$$

$$V(\infty) = V_y(\infty) = 0 \quad (68)$$

where the subscripts denote differentiation. Note that the conditions expressed by equation (68) replace the boundary conditions at the second wall and require that influences of one wall do not affect the other. Thus y can be considered as the coordinate normal to the first (or left-hand) wall (that is, the one corresponding to $Y = 0$) and $-y$ will be the coordinate normal to the other wall, which is at $Y = d$. Hence, use should be made of the proper part of equation (67) in each solution.

From equation (65) it can be seen that the frictional heating effects will be negligible for large Ra unless CK_A/Ra (or $C\gamma\beta f_X d/c_p$) is at least of unit order of magnitude. It should perhaps be pointed out here, in contradistinction to the qualitative discussions in references 1 and 12, that the frictional heating is important only if essentially the ratio of K (based on any appropriate temperature) to Ra is of unit order of magnitude or larger, as can, in fact, be verified in general. Thus it should be noted that the discussions in those references hold specifically only if Ra is of unit order or smaller or if Ra does not appear as an explicit parameter of the problem (as in ref. 1, for example). For the range of conditions and physical properties of fluids being considered, it is unlikely that CK_A/Ra will be of unit order for a flow generated in a gravitational field alone with large Ra . Therefore, unless the natural-convection flow is being generated by a body force considerably stronger than gravity, the ratio of the volumetric expansion coefficient to the specific heat at constant pressure is unusually large, or there is considerable forced flow (to increase C), the frictional heating effects will not be important for large Ra . (Of course, the possibility always exists that some unusual fluid will be employed whose physical properties are such that CK_A/Ra will be of such a magnitude that the frictional heating effects will be important for large Ra even in a gravitational field. Liquids near their critical state may be representative in this respect (see ref. 13)). Furthermore, it can be seen

from the same equation that the effects of the heat sources will be important only if $\alpha/CRa^{1/2}$ is of unit order of magnitude for large Ra . This is physically reasonable.

Since the frictional heating effects are negligible for large Ra , unless CK_A is very large these effects will be neglected in this section. (A method of successive approximations similar to that described in the previous sections could be applied without difficulty to eq. (65) if these effects are of consequence.) Therefore, letting

$\bar{V} = V - \alpha/CRa^{1/2}$, equations (65) to (68) become, respectively,

$$\bar{V}_{yyyy} + \bar{V} = 0 \quad (69)$$

$$\bar{V}(0) = -\frac{\alpha}{CRa^{1/2}} \quad (70)$$

$$\bar{V}_{yy}(0) = \bar{m} \quad (71)$$

$$\bar{V}(\infty) = \bar{V}_{yy} = 0 \quad (72)$$

The solution satisfying equations (69) to (72) is

$$\bar{V} = -e^{-\bar{y}/\sqrt{2}} \left(\bar{m} \sin \frac{\bar{y}}{\sqrt{2}} + \frac{\alpha}{CRa^{1/2}} \cos \frac{\bar{y}}{\sqrt{2}} \right) \quad (73)$$

To find the temperature distribution the second derivative of equation (73) is necessary, and this is given by

$$\bar{V}_{yy} = -e^{-\bar{y}/\sqrt{2}} \left(\frac{\alpha}{CRa^{1/2}} \sin \frac{\bar{y}}{\sqrt{2}} - \bar{m} \cos \frac{\bar{y}}{\sqrt{2}} \right) \quad (74)$$

For large values of the Rayleigh number Ra , then, the dimensionless velocity and temperature distributions are given by

$$u_a = \frac{CK_A}{Ra^{1/2}} \left(\bar{V} + \frac{\alpha}{CRa^{1/2}} \right) \quad (75)$$

and

$$\tau_a = CK_A (1 - \bar{V}_{yy}) \quad (76)$$

Solution of Special Case Simulating an Enclosed Channel

There is considerable interest in the natural-convection flow in a completely enclosed rectangular region. In reference 7, the natural-convection flow of fluids containing heat sources between two parallel planes is considered (as is the case here also); but there, in order to simulate an enclosed rectangular region, it is further specified that the net mass flow be zero and that the walls be at the same temperature. This problem is treated in an approximate manner in reference 7 in that the velocity distribution was postulated without regard to the equations of motion and, hence, it would be desirable for comparison purposes to obtain a more exact solution for this special case from the solutions found herein.

For zero net mass flow in the channel the parameter C can be determined directly from the other parameters of the problem and equation (58). Thus

$$C_0^0 = \frac{\theta_{w1}}{2Ad} + \frac{\alpha}{\sqrt{2} Ra^{1/4}} \left(\frac{\cosh 2r + \cos 2r}{\sin 2r - \sinh 2r} \right) \left[\frac{\sqrt{2}}{Ra^{1/4}} \left(\frac{\sin 2r + \sinh 2r}{\cosh 2r + \cos 2r} \right) - 1 \right] \quad (77a)$$

where the superscript denotes the zero net mass flow and the subscript designates the order of the approximation. It is interesting to note from this equation that for no internal heat sources ($\alpha = 0$), zero net mass flow in the channel can be obtained when $C = \theta_{w1}/2Ad$. However, to obtain the solution for the special case simulating flow with heat sources in a completely enclosed region with walls of equal temperatures from the solutions presented in the previous sections, θ_{w1} must be zero in equation (77a), and therefore

$$C_0^0 = \frac{\alpha}{\sqrt{2} Ra^{1/4}} \left(\frac{\cosh 2r + \cos 2r}{\sin 2r - \sinh 2r} \right) \left[\frac{\sqrt{2}}{Ra^{1/4}} \left(\frac{\sin 2r + \sinh 2r}{\cosh 2r + \cos 2r} \right) - 1 \right] \quad (77b)$$

The velocity and temperature distributions for this special case are then obtained by replacing C in equations (52) and (54) by C_0^0 as given by equation (77b). Further physical significance of the zero net mass flow case can be inferred from equation (13). Integration of this equation over the channel cross section shows that for no net mass flow all the heat generated internally (by heat sources and by aerodynamic heating if the latter is significant) in a given cross section must be transferred to the walls.

Computations made for this case including frictional heating yielded no appreciable deviations from the zeroth-order results.

Solutions for Case of Convective Inversion

An interesting aspect associated with the natural-convection phenomenon is that the Grashof number can change sign; this implies a reversal in the flow direction and is referred to as convective inversion (see p. 109, ref. 8). The sign of the modified Grashof number in the present paper can be changed in one of three ways: (1) by a change of the sign of the longitudinal temperature gradient $\partial T / \partial X = A$, (2) by a change in the direction of the generating body force, and (3) by a change in the sign of the volumetric expansion coefficient as occurs near the critical state of a liquid (see ref. 13).

Since the modified Grashof number appears in the parameters K_A and Ra connected with the problem considered herein, the effects of sign changes of the Grashof number in the solutions should be studied. From its definition, K_A is proportional to A , f_X^2 , and β^2 so that only the first will alter its sign. Note further, however, that the modified Rayleigh number Ra is essentially the product of the Prandtl number and a modified Grashof number, that is, a Grashof number which depends on the product (Ad) of the longitudinal temperature gradient and the distance between the plates. Hence, any one of (1), (2), or (3) given in the preceding paragraph will lead to a change in the sign of Ra . For negative Ra the solutions as given in the previous sections do not apply, and hence the foregoing boundary-value problem (eqs. (22) to (25)) would have to be solved with negative Ra . These solutions can be readily obtained, but it is found that with frictional heating neglected these solutions change character with changes in Ra and that there exist critical negative values of Ra for which the solutions become meaningless. In an attempt to explain these unusual results, further interpretation of the problem must be made. Reexamination of the meaning of negative Ra shows that not only changes in the body force direction and sign of the volumetric expansion coefficient but also a change in the sign of the longitudinal temperature gradient A can lead to negative Ra . If the negative Ra is attributed to the last cause, the physical interpretation of the unusual mathematical results pointed out becomes clearer, because a negative A implies that the fluid is being heated from below and this situation leads to a "Rayleigh-type" instability of natural-convection flows due to the "piling of heavy fluid on lighter fluid." Analogous interpretations, of course, also follow directly for changes in the body force direction and in the sign of the volumetric expansion coefficients. Natural-convection flows heated from below between horizontal plates have been studied experimentally in some detail (see refs. 8, 14, and 15, for example), and it was found that the flow does indeed change character (into cellular

motion) for certain critical values of the Rayleigh number. Hence, it is believed that the critical values of Ra found from the linearized analysis (in that the aerodynamic heating was neglected) for negative Ra may be analogous to those observed in actual cases. However, since this instability leads to these additional complications and should be further investigated (perhaps using the true nonlinear eqs.), the case of negative Ra will not be treated further herein. It should, however, be kept in mind that if in an actual case of the configuration considered herein the Ra is negative, the flow and heat transfer will not be as predicted in this paper but should be expected to exhibit a behavior pertinent to the "unstable-type" flows.

RESULTS AND DISCUSSION

Velocity and Temperature Distributions

The relations between the actual and dimensionless velocities and temperatures as determined from the various transformations in the analysis (see eqs. (16)) are

$$U = \sqrt{\frac{c_p Ad}{Pr K_A}} u \quad (78)$$

$$\theta = \frac{Ad}{K_A} \tau \quad (79)$$

where U and θ denote the actual and u and τ , the dimensionless quantities. For a given fluid, configuration, heat-source intensity, and mass flow, the velocity and temperature distributions can be computed from equations (52) to (55) (for $Ra > 0$); and for zero net mass flow and the walls of the same temperature, by applying equation (77b) to equations (52) and (55). These computations will be accurate within the limits of the method of solution; that is, for moderate and small values of Ra the solutions yield results of reasonable accuracy for small CK_A , and for large Ra the zeroth-order approximations or, even more simply, the asymptotic solutions will give answers valid for all CK_A . The range of applicability of the various solutions presented herein will be discussed more fully subsequently.

Because the solutions were obtained in the convenient forms (eqs. (52) and (54), for example) wherefrom the qualitative effects of the various parameters associated with the problem can be studied, and since

tabular values of the universal functions are presented to facilitate computations for any specific case, no extensive detailed calculations will be given covering the entire range of values taken on by the parameters. Representative velocity and temperature profiles were, however, calculated for $K_A = 10$, $m = -1, 1$, and 2 , $\alpha = 0, 10$, and 100 , and $Ra = 10, 10^2, 1600$, and 10^4 . In addition, the parameter C was given the value -1 in all the computations except those for the case simulating flow in a completely enclosed region. In this way the relative influences of the other parameters are just as apparent, but the number of computations is greatly reduced. The results of these computations are presented in figures 2 to 9. The contents of each specific figure (numbers 2 to 9) are listed in the following table:

$K_A = 10$		u_0, u_1				τ_0, τ_1			
m	α	$Ra = 10$	10^2	1600	10^4	10	10^2	1600	10^4
-1	0	2(a)	3(a)	4(a)	5(a)	6(a)	7(a)	8(a)	9(a)
	10	2(a)	3(a)	4(a)	5(a)	6(a)	7(a)	8(a)	9(a)
	100	2(a)	3(a)	4(a)	5(a)	6(a)	7(a)	8(a)	9(a)
1	0	2(b)	3(b)	^a 4(b)	5(b)	6(b)	7(b)	^a 8(b)	9(b)
	10	^{a,b} 2(b)	3(b)	4(b)	5(b)	^{a,b} 6(b)	7(b)	8(b)	9(b)
	100	2(b)	3(b)	4(b)	5(b)	6(b)	7(b)	8(b)	9(b)
2	0	^{a,b} 2(c)	3(c)	4(c)	^c 5(c)	^{a,b} 6(c)	7(c)	8(c)	^c 9(c)
	10	2(c)	3(c)	4(c)	5(c)	6(c)	7(c)	8(c)	9(c)
	100	2(c)	3(c)	4(c)	^c 5(c)	6(c)	7(c)	8(c)	^c 9(c)

^aIncludes results for u or τ .

^bIncludes results for $u(2)$ or $\tau(2)$.

^cIncludes results for u_a or τ_a .

For each triplet of parametric values (m, α, Ra) the profiles were computed with frictional heating neglected (by eqs. (52) and (54) and denoted by u_0 and τ_0 on the figs.), with frictional heating included to a first approximation (by eqs. (53) and (55) and denoted by u_1 and τ_1), and in several specific cases with frictional heating completely accounted for (by numerical solution of eqs. (22) to (25) using a Card-Programmed Electronic Calculator and denoted by u and τ). For

$Ra = 10^4$ the asymptotic solutions (given by eqs. (75) and (76) and denoted by u_a and T_a) are also included for $K_A = 10$, $m = 2$, and $\alpha = 0$ and 100. The asymptotic solutions were computed from each individual wall to the channel center and then faired in to join smoothly. From these computations any qualitative trends obtained by examination of the solutions can be further substantiated and, in addition, some definition of the range in which the frictional or aerodynamic heating exerts a large influence can be made. Calculations were also made for the special case simulating a completely enclosed region in which there is no net mass flow and the walls are at the same temperature by applying equation (77) to the appropriate solutions. These curves are given in figures 10 and 11. The velocity and temperature profiles (particularly for $Ra \leq 10^4$) are qualitatively similar to those determined experimentally in reference 16.

Effect of different wall-temperature configurations (m varying) and heat sources (α varying). - From equations (52) to (55) and their related universal functions, it can be seen, as expected, that an increase in the wall temperature parameter m or an increase in the heat-source parameter α results in larger velocities and higher temperatures. These trends together with that of increasing net mass flow, as represented by the area under the u -curves, with m and α can be observed on figures 2 to 9. It can also be seen from figures 6 to 9 that if sufficient heat is generated by the heat sources, the direction of heat transfer will be changed. In agreement with the statements made in the section dealing with the zero net mass-flow case, note from figures 2(a), 3(a), 4(a), and 5(a) that if aerodynamic heating is neglected for $m = -1$ (since $C = -1$) and $\alpha = 0$, there is no net mass flow. In general, the velocity distributions become more symmetrical with the larger α (see figs. 2(a), 3(a), 4(a), and 5(a), for example) because the heat added uniformly by the heat sources counteracts any asymmetry imposed by the wall thermal conditions.

Effect of the modified Rayleigh number (Ra). - Examination of the solutions (eqs. (52) to (55)) shows that the velocities and temperatures decrease with increasing values of the modified Rayleigh number Ra . This trend can also be seen by comparison of corresponding curves in figures 2 to 9, and even by comparing with the curves in reference 1 which are for $Ra = 0$. For large Ra it can be seen from figures 5(b), 5(c), 9(b), and 9(c) that the velocity and temperature profiles take on a "boundary-layer form." Asymptotic solutions computed for $Ra = 10^4$, $K_A = 10$, $m = 2$, and $\alpha = 0$ and 100 are also presented on figures 5(c) and 9(c), and these very closely approximate the more exact solutions. Hence, for large Ra the asymptotic solutions can be employed to yield reasonable results much more simply. For the case

where $m = -1$ and $\alpha = 0$, increasing the modified Rayleigh number changes the temperature distribution from essentially the conduction profile (that is, an almost linear distribution) at $Ra = 10$; the increased effect of the convection is then apparent for the larger values of the Rayleigh number. It is interesting to note that for $K_A = 10$, $\alpha = 10$, and $m = -1, 1$, and 2 , changes in the Rayleigh number can so affect the temperature distributions that the heat flow direction from one or both the walls can be altered. (Compare corresponding parts of figs. 6 to 9.) This point will be more graphically portrayed in the subsequent discussion of Nusselt numbers.

The velocity and temperature distributions (see figs. 10 and 11) for the special case considered herein of zero net mass flow and walls at the same temperature are not in general appreciably altered in shape by increases in Ra although the velocity peaks vary inversely with the Rayleigh number. The shape of the velocity and temperature profiles is seen to be qualitatively the same as that assumed in reference 7.

Effect of frictional heating. - By comparing the profiles presented in figures 2 to 9 computed by neglecting frictional heating (denoted by the subscript zero) with those computed including the aerodynamic heating to a first order (denoted by the subscript unity), the effect of the aerodynamic heating on the velocities and temperatures can be studied. Numerical solutions obtained of the complete boundary-value problem (eqs. (22) to (25)) in which the frictional heating was entirely taken into account are also included (with no subscripts) (see preceding table) on figures 2(b), 2(c), 4(b), 6(b), 6(c), 8(b), 10, and 11 for comparisons with the approximate solutions.

In accord with the discussion on the asymptotic solutions, it can be seen that when K_A is small compared with Ra (recall that $C = -1$ in these calculations) the aerodynamic heating effects are negligible. Since no computations were made herein for $K_A > 10$, the computations made for $Ra = 1600$ and 10^4 show no deviation between the zeroth and first approximations, and these are also coincident with the numerical solution (see figs. 4(b) and 8(b)). Hence, in the range $K_A/Ra \ll 1$, the zeroth-order approximations will yield accurate results; if, in addition, $Ra \gg 1$, the asymptotic solutions provide a simple means of obtaining the velocity and temperature profiles. Note that the parameter K_A serves merely as a scale factor in the zeroth-order solutions.

In the range where K_A and the Rayleigh number are of the same order of magnitude, the frictional heating affects the results to greater or lesser degree depending on the particular amount of heat addition as specified essentially by the parameters m and α (figs. 2, 3, 6, and 7) and, hence, the first-order approximations should be employed in

this range. Comparison of the first-order solutions with the several numerical solutions of the entire boundary-value problem shows close agreement for the cases computed. Hence, unless the conditions are more severe than the most extreme conditions for the range of parameters considered herein as represented by $K_A/Ra = 1$, $m = 2$, and $\alpha = 100$, the first-order solutions will yield results which include the effect of aerodynamic heating of reasonable accuracy. In this range where its effects are important, this frictional heat, of course, acts just as do the heat sources and leads to increased velocities and altered temperature profiles and, consequently, different heat-transfer rates (figs. 2, 3, 6, and 7).

For the special case simulating flow in a completely enclosed region, the aerodynamic heating did not affect the results appreciably over the range of parameters under consideration. A numerical solution completely including the effects of aerodynamic heating was made for $Ra = 10$; it can be seen in figures 10 and 11 that this solution coincides with the zeroth-order solution, which neglects the effect of frictional heating.

The complete consideration of frictional heating (as in the numerical solutions) for the problem discussed herein, just as for the case (essentially $Ra = 0$) reported in reference 1, leads to the two results (a) that there exists a critical set of conditions beyond which no solutions exist, and (b) that where solutions exist there are two solutions for every set of admissible parametric values. Examples of these second solutions are presented in figures 2(b), 2(c), 6(b), and 6(c) (denoted by $u(2)$ and $\tau(2)$), and it can be seen that the velocities are more than 10 times as large as the first solutions and the temperatures are much greater than the corresponding first solution temperatures. These last unusual results cannot be predicted from the solutions obtained by successive approximations as described herein, but are found from numerical solutions obtained by means of a Card-Programmed Electronic Calculator. At present the significance of the second solutions is not explained, although it is felt that they are intimately connected with the unique regenerative action of the frictional heating in natural convection. The existence of the critical conditions appears to be similar to the thermal choking phenomenon.

HEAT TRANSFER

Nusselt Numbers

The heat-transfer coefficients for the natural-convection phenomenon treated here can be expressed in terms of Nusselt numbers. The Nusselt number is here defined as

$$Nu \equiv \frac{hd}{k} = \frac{1}{A} \left(\frac{\partial T^*}{\partial Y} \right)_{0,d}$$

where the double subscript signifies that the temperature gradient is to be evaluated at either $Y = 0$ or $Y = d$, depending on the wall under consideration.

In terms of the dimensionless quantities,

$$Nu = \frac{1}{K_A} \left(\frac{dT}{dy} \right)_{0,1} \quad (80)$$

The temperature gradient can be found from the zeroth-order solutions, and the Nusselt numbers can be computed on this basis from

$$Nu_{00} = \frac{1}{2\sqrt{2} Ra^{1/4}} \left\{ \frac{1}{\cosh^2 r + \cos^2 r - 1} \left[\alpha(\sinh 2r + \sin 2r) + \frac{C(m+1)Ra^{1/2}}{2} (\sinh 2r - \sin 2r) \right] + \frac{C(m-1)Ra^{1/2}}{2(\cos^2 r - \cosh^2 r)} (\sinh 2r + \sin 2r) \right\} \quad (81)$$

$$Nu_{01} = \frac{1}{2\sqrt{2} Ra^{1/4}} \left\{ \frac{-1}{\cosh^2 r + \cos^2 r - 1} \left[\alpha(\sinh 2r + \sin 2r) + \frac{C(m+1)Ra^{1/2}}{2} (\sinh 2r - \sin 2r) \right] + \frac{C(m-1)Ra^{1/2}}{2(\cos^2 r - \cosh^2 r)} (\sinh 2r + \sin 2r) \right\} \quad (82)$$

where the first subscript denotes that zeroth-order approximation is used, and the second denotes the wall with which the Nusselt number is associated. (Eqs. (81) and (82) are, of course, specifically for Ra positive.) Note that these zeroth-order Nusselt numbers are independent of K_A . When CK_A is of the same order of magnitude as Ra , the zeroth-order approximation has been shown to be inaccurate; therefore improved Nusselt numbers can be obtained by using the appropriate τ (first-order approximation) solutions and, for the same conditions as for equations (81) and (82), the Nusselt numbers can be computed from

$$Nu_{10} = Nu_{00} + \frac{K_A}{64\sqrt{2} Ra^{7/4}} \left[\alpha^2 \Omega_1 - C\alpha Ra^{1/2} (m+1) \Omega_2 + \frac{C^2(m-1)^2 Ra}{4} \Omega_3 + \frac{C^2(m+1)^2 Ra}{4} \Omega_4 + C(m-1)\alpha Ra^{1/2} \Omega_5 - \frac{C^2(m^2-1)}{2} Ra \Omega_6 \right] \quad (83)$$

$$\begin{aligned}
 Nu_{11} = Nu_{01} - \frac{K_A}{64\sqrt{2} Ra^{7/4}} \left[\alpha^2 \Omega_1 - C \alpha Ra^{1/2} (m+1) \Omega_2 + \frac{C^2 (m-1)^2 Ra}{4} \Omega_3 \right. \\
 \left. + \frac{C^2 (m+1)^2 Ra}{4} \Omega_4 + C (m-1) \alpha Ra^{1/2} \Omega_5 + \frac{C^2 (m^2-1)}{2} Ra \Omega_6 \right] \quad (84)
 \end{aligned}$$

where the various Ω_i in equations (83) and (84) are given by equations (B43) to (B48) in appendix B.

Computations of the Nusselt numbers were made over a range of values of Ra from equations (81) to (84) for $K_A = 10$, $m = -1, 1$, and 2 , and $\alpha = 0$ and 10 where again C was taken to be -1 , and the results are presented in figures 12 and 13 for the wall at $Y = 0$ and $Y = d$, respectively. The figures show that for the wall at $Y = 0$ the Nusselt numbers decrease, in general, with increasing Ra , and for the wall at $Y = d$ the Nusselt numbers increase with the modified Rayleigh number except for the case where $m = -1$. For $K_A = 10$ and $\alpha = 10$, the Nusselt number changes sign with increases in Ra because of the variation of the temperature profile with Ra , as was previously noted.

Figures 12 and 13 also demonstrate clearly the effect of the aerodynamic or frictional heating. This effect, in accordance with all that preceded, is extremely pronounced for low values of the Rayleigh number (that is, when K/Ra is of unit order of magnitude).

Flow in an enclosed region. - For the special case simulating flow in a completely enclosed region ($M = 0$, $m = 1$, and $\alpha \neq 0$), the calculations for the temperature profile were extended over a larger range of Ra and plotted in figure 14 as the ratio Φ of the temperature difference to that for pure conduction, as was done in reference 7. The conduction temperature difference used in Φ is the channel center-to-wall difference subject to uniform heat generation by sources and is equal to $\alpha K_A/8$. The temperature profiles computed in an approximate manner in reference 7 are compared with those computed more exactly by the method reported in this paper, and it can be seen that the discrepancy becomes quite apparent for values of $Ra = 10^4$ and above.

The N_I in reference 7 is related to Ra by $Ra = \frac{1}{\gamma} N_I$; hence, for most liquids N_I and Ra are identical. If $\gamma \neq 1$, γ is merely a scale factor. It can be seen from figure 14 that for $Ra < 10^4$, the temperature gradients at the wall are all almost identical, and hence, even if the temperature profiles themselves were not identical, the heat transfer computed by the two methods would be in reasonable agree-

ment. The variations of the dimensionless temperature variable Φ_0 (ratio of center-to-wall temperature difference to that for pure conduction) as used in reference 7 with Ra as given by the two methods are also compared in figure 15, and hence the quantitative limits of the approximate method can be seen.

CONCLUDING REMARKS

An analysis was made of the flow subject to body forces between two parallel plane surfaces oriented in the direction of the generating body force along which the temperature is specified to vary linearly. The solutions for natural convection and those for combined natural and forced convection were found to be essentially the same. It was found that a modified Rayleigh number (product of Prandtl and modified Grashof numbers) in addition to the parameter K_A was of significance in this problem. Solutions for the velocity and temperature distributions are given in terms of "universal" tabulated functions. Detailed velocity and temperature profiles were computed and it was found that, in general, the velocity and temperature differences increase with the wall temperature parameter and with additional heat due to heat sources. The velocities and temperatures decrease with increasing values of the modified Rayleigh number. When the ratio of CK_A to the modified Rayleigh number is of unit order of magnitude, the frictional or aerodynamic heating appreciably affects the velocity and temperature distributions. Asymptotic solutions for large Ra are presented which make computations in this range relatively simple. For any given set of the parameters, complete consideration of frictional heating implied the existence of two flow and heat-transfer states and implied that no solution exists beyond certain critical values.

Consideration was given to a special case simulating the natural-convection flow of fluids with heat sources in a completely enclosed region with the walls at the same temperature. Computations from the solutions for this special case demonstrated that an approximate method developed in another paper should yield reasonably accurate results as long as the modified Rayleigh number is less than 10^4 . The effects of aerodynamic heating were found to be negligible for this case.

Study of the convective inversion aspect of the present problem led to the inference that for negative values of the Rayleigh number, additional complications arise because of an instability (due to heating from below) of the flow which must be more thoroughly investigated.

Lewis Flight Propulsion Laboratory
National Advisory Committee for Aeronautics
Cleveland, Ohio, December 29, 1953

APPENDIX A

SYMBOLS

The following notation is used in this report:

A	longitudinal temperature gradient
a_i	constants in eq. (39); $i = 1, 2, 3, 4$
B_i	constants defined by eqs. (B14) to (B35); $i = 1, 2, 3, \dots, 22$
C	constant in eq. (17)
C_i	constants defined by eqs. (B36); $i = 1, 2, 3, \dots, 6$
C_0^0	constant defined by eq. (77b)
\bar{C}	constant in eq. (14b)
c_p	specific heat at constant pressure
c_v	specific heat at constant volume
D_i	constants defined by eqs. (B37); $i = 1, 2, 3, \dots, 10$
d	characteristic length (specifically distance between plates)
E	constant defined by eq. (50)
E_i	constants defined by eqs. (B38); $i = 1, 2, 3, \dots, 6$
e	constant, $(i+1)$
F	constant defined by eq. (51)
f_X	negative of X-component of body force per unit mass
G	Green's function
Gr_A	modified Grashof number, $\beta f_X Ad^4/\nu^2$
g	constant, $(i-1)$

h	heat-transfer coefficient
h_i	constants defined by eq. (B39); $i = 1, 2, 3, 4$
J	constant, $Ra^{1/2}CK_A/64$
K_A	dimensionless parameter, $Pr Gr_A \frac{\beta r_X d}{c_p}$
k	thermal-conductivity coefficient
L_i	constants defined by eqs. (B40); $i = 1, 2$
M	dimensionless mass flow
M_i	constants defined by eqs. (B41); $i = 1, 2, 3, 4$
m	constant defined by eq. (25)
\bar{m}	constant defined by eq. (64)
Nu	Nusselt number, hd/k
N_I	modified Rayleigh criterion as given in ref. 6, γRa
P	pressure
Pr	Prandtl number, $c_p \mu / k$
Q	heat due to heat sources
Q_i	constants defined by eqs. (B42); $i = 1, 2, 3, \dots, 8$
R	constant, $Ra/16$
Ra	modified Rayleigh number, $\frac{1}{\gamma} Pr Gr_A$
r	constant, $R^{1/4}/\sqrt{2}$
T, T^*	temperature
U	velocity
u	dimensionless velocity
\bar{u}	dimensionless velocity, u/CK_A

V	dimensionless velocity defined by eq. (61)
\bar{V}	dimensionless velocity, $V - \frac{\alpha}{cRa^{1/2}}$
v	dimensionless velocity, $\bar{v}/64$
\bar{v}	dimensionless velocity defined by eq. (26)
X	longitudinal coordinate
Y	transverse coordinate
y	dimensionless transverse coordinate
\bar{y}	dimensionless transverse coordinate, $Ra^{1/4}y$
α	dimensionless heat-source parameter, Qd/kA
β	coefficient of volumetric expansion, $\rho \left[\frac{\partial(1/\rho)}{\partial T} \right]_p$
γ	ratio of specific heats
η	dimensionless coordinate, $2y - 1$
θ	temperature difference, $T - T_{w0}$
λ	constant, $-\alpha K_A/64$
μ	absolute viscosity coefficient
ν	kinematic viscosity coefficient
ξ	dummy variable
ρ	density
τ	dimensionless temperature difference
Φ	dimensionless temperature difference, $8\tau/\alpha K_A$
Φ_0	dimensionless center-to-wall temperature difference, $8(\tau)_{y=1/2}/\alpha K_A$
Ω_i	constants in eqs. (80) and (81); $i = 1, 2, 3, \dots, 6$

Subscripts:

a asymptotic solution
ca complementary antisymmetric solution
cs complementary symmetric solution
I inviscid solution
n order of approximation
P particular solution
w₀ conditions at $y = 0$
w₁ conditions at $y = 1$
0 zeroth-order approximation
1 first-order approximation

Superscript:

(2) second flow and heat-transfer state

APPENDIX B

FIRST-ORDER SOLUTIONS

The explicit forms of the first-order solutions to be used in equation (46) are:

$$v_{10} = \frac{1}{Ra^{3/2}} [B_1 \cosh r\eta \cos r\eta + B_2 \sinh r\eta \sin r\eta + B_3 \cosh 2r\eta \cos 2r\eta + B_4 \sinh 2r\eta \sin 2r\eta + B_5 (\cos 2r\eta - \cosh 2r\eta) + 15 B_3] \quad (B1)$$

$$v_{11} = \frac{1}{Ra^{3/2}} [B_6 \cosh r\eta \cos r\eta + B_7 \sinh r\eta \sin r\eta - B_4 \cosh 2r\eta \cos 2r\eta + B_3 \sinh 2r\eta \sin 2r\eta - 15 B_4] \quad (B2)$$

$$v_{12} = \frac{1}{Ra^{3/2}} [B_8 \cosh r\eta \cos r\eta + B_9 \sinh r\eta \sin r\eta + B_{10} \cosh 2r\eta \cos 2r\eta + B_{11} \sinh 2r\eta \sin 2r\eta + B_{12} (\cosh 2r\eta + \cos 2r\eta) - 15 B_{10}] \quad (B3)$$

$$v_{13} = \frac{1}{Ra^{3/2}} [B_{13} \cosh r\eta \cos r\eta + B_{14} \sinh r\eta \sin r\eta - B_3 \cosh 2r\eta \cos 2r\eta - B_4 \sinh 2r\eta \sin 2r\eta + B_5 (\cos 2r\eta - \cosh 2r\eta) - 15 B_3] \quad (B4)$$

$$v_{14} = \frac{1}{Ra^{3/2}} [B_{15} \sinh r\eta \cos r\eta + B_{16} \cosh r\eta \sin r\eta + B_{17} \sinh 2r\eta \cos 2r\eta + B_{18} \cosh 2r\eta \sin 2r\eta + B_{19} \sin 2r\eta + B_{20} \sinh 2r\eta] \quad (B5)$$

$$v_{15} = \frac{1}{Ra^{3/2}} \left[B_{21} \sinh r\eta \cos r\eta + B_{22} \cosh r\eta \sin r\eta \right. \\ \left. - B_{18} \sinh 2r\eta \cos 2r\eta + B_{17} \cosh 2r\eta \sin 2r\eta \right. \\ \left. + B_{20} \sin 2r\eta - B_{19} \sinh 2r\eta \right] \quad (B6)$$

The constants B_i ($i = 1, 2, \dots, 22$) appearing in the preceding equations are readily computed for a given Ra . In the subsequent section of this appendix these constants are written explicitly in a form suitable for reasonably rapid computation.

The second derivatives appearing in equations (54) and (55) are

$$v''_{01} = \frac{-Ra^{1/2}}{4(\cos^2 r - \cosh^2 r)} \left[\cosh r \sin r \cosh r\eta \sin r\eta \right. \\ \left. + \sinh r \cos r \sinh r\eta \cos r\eta \right] \quad (B7)$$

$$v''_{10} = \frac{1}{4Ra} \left[B_2 \cosh r\eta \cos r\eta - B_1 \sinh r\eta \sin r\eta \right. \\ \left. + 4B_4 \cosh 2r\eta \cos 2r\eta - 4B_3 \sinh 2r\eta \sin 2r\eta \right. \\ \left. - 2B_5(\cos 2r\eta + \cosh 2r\eta) \right] \quad (B8)$$

$$v''_{11} = \frac{1}{4Ra} \left[B_7 \cosh r\eta \cos r\eta - B_6 \sinh r\eta \sin r\eta \right. \\ \left. + 4B_3 \cosh 2r\eta \cos 2r\eta + 4B_4 \sinh 2r\eta \sin 2r\eta \right] \quad (B9)$$

$$v''_{12} = \frac{1}{4Ra} \left[B_9 \cosh r\eta \cos r\eta - B_8 \sinh r\eta \sin r\eta \right. \\ \left. + 4B_{11} \cosh 2r\eta \cos 2r\eta - 4B_{10} \sinh 2r\eta \sin 2r\eta \right. \\ \left. + 2B_{12}(\cosh 2r\eta - \cos 2r\eta) \right] \quad (B10)$$

$$v''_{13} = \frac{1}{4Ra} \left[B_{14} \cosh r\eta \cos r\eta - B_{13} \sinh r\eta \sin r\eta \right. \\ \left. - 4B_4 \cosh 2r\eta \cos 2r\eta + 4B_3 \sinh 2r\eta \sin 2r\eta \right. \\ \left. - 2B_5(\cos 2r\eta + \cosh 2r\eta) \right] \quad (B11)$$

$$\begin{aligned}
 v''_{14} = \frac{1}{4Ra} & \left[-B_{15} \cosh r\eta \sin r\eta + B_{16} \sinh r\eta \cos r\eta \right. \\
 & - 4B_{17} \cosh 2r\eta \sin 2r\eta + 4B_{18} \sinh 2r\eta \cos 2r\eta \\
 & \left. - 2B_{19} \sin 2r\eta + 2B_{20} \sinh 2r\eta \right] \quad (B12)
 \end{aligned}$$

$$\begin{aligned}
 v''_{15} = \frac{1}{4Ra} & \left[-B_{21} \cosh r\eta \sin r\eta + B_{22} \sinh r\eta \cos r\eta \right. \\
 & + 4B_{18} \cosh 2r\eta \sin 2r\eta + 4B_{17} \sinh 2r\eta \cos 2r\eta \\
 & \left. - 2B_{20} \sin 2r\eta - 2B_{19} \sinh 2r\eta \right] \quad (B13)
 \end{aligned}$$

Constants for First-Order Approximation

The constants appearing in equations (B1) to (B13) are written in an expeditious form for computing as follows:

$$\begin{aligned}
 B_1 = -\frac{4}{L_1} & \left[(-3D_1 + D_2)E_1 + (D_3 - 3D_4)E_2 + 2(D_3 + D_4)E_3 + 2(D_1 + D_2)E_4 \right. \\
 & \left. + (D_3 + D_4)E_5 - (D_1 + D_2)E_6 \right] + \frac{512}{15} \frac{h_1 h_2}{M_1} \quad (B14)
 \end{aligned}$$

$$\begin{aligned}
 B_2 = -\frac{4}{L_1} & \left[(D_3 - 3D_4)E_1 + (3D_1 - D_2)E_2 + 2(D_1 + D_2)E_3 - 2(D_3 + D_4)E_4 \right. \\
 & \left. - (D_1 + D_2)E_5 - (D_3 + D_4)E_6 \right] - \frac{128}{15} \frac{(2h_1^2 + h_2^2)}{M_1} \quad (B15)
 \end{aligned}$$

$$B_3 = -\frac{32}{15} \frac{h_1 h_2}{M_1} \quad (B16)$$

$$B_4 = \frac{16}{15} \frac{(h_1^2 - h_2^2)}{M_1} \quad (B17)$$

$$B_5 = -\frac{16}{5} \frac{(h_1^2 + h_2^2)}{M_1} \quad (B18)$$

$$\begin{aligned}
 B_6 = \frac{4}{L_1} & \left[(3D_1 - D_2)E_2 + (D_3 - 3D_4)E_1 + (D_3 + D_4)E_6 + (D_1 + D_2)E_5 \right. \\
 & \left. - \frac{256}{15M_1} (h_2^2 - h_1^2) \right] \quad (B19)
 \end{aligned}$$

$$B_7 = \frac{4}{L_1} \left[(-D_3 + 3D_4)E_2 + (3D_1 - D_2)E_1 - (D_1 + D_2)E_6 + (D_3 + D_4)E_5 \right] + \frac{128 h_1 h_2}{15M_1} \quad (B20)$$

$$B_8 = -\frac{4}{L_2} \left[(D_5 - D_6 - 2D_4)C_1 + (2D_1 + D_7 - D_8)C_2 - 2(D_5 + D_6)C_3 - 2(D_7 + D_8)C_4 \right. \\ \left. + (D_5 - D_6 + 2D_4)C_5 + (-2D_1 + D_7 - D_8)C_6 \right] + \frac{448 h_1 h_2}{15M_2} - \frac{32(M_5 + M_4)}{5M_2} \quad (B21)$$

$$B_9 = -\frac{4}{L_2} \left[(2D_1 + D_7 - D_8)C_1 + (-D_5 + D_6 + 2D_4)C_2 - 2(D_7 + D_8)C_3 + 2(D_5 + D_6)C_4 \right. \\ \left. + (-2D_1 + D_7 - D_8)C_5 + (-D_5 + D_6 - 2D_4)C_6 \right] + \frac{64(M_5 - M_4)}{15M_2} \quad (B22)$$

$$B_{10} = \frac{32 h_1 h_2}{15M_2} \quad (B23)$$

$$B_{11} = -\frac{16(M_5 - M_4)}{15M_2} \quad (B24)$$

$$B_{12} = \frac{16(M_5 + M_4)}{5M_2} \quad (B25)$$

$$B_{13} = \frac{4}{L_1} \left[(-3D_1 + D_2)E_1 + (D_3 - 3D_4)E_2 - 2(D_3 + D_4)E_3 - 2(D_1 + D_2)E_4 \right. \\ \left. + (D_3 + D_4)E_5 - (D_1 + D_2)E_6 \right] - \frac{512 h_1 h_2}{15M_1} \quad (B26)$$

$$B_{14} = \frac{4}{L_1} \left[(D_3 - 3D_4)E_1 + (3D_1 - D_2)E_2 - 2(D_1 + D_2)E_3 + 2(D_3 + D_4)E_4 - (D_1 + D_2)E_5 \right. \\ \left. - (D_3 + D_4)E_6 \right] - \frac{128}{15M_1} \left[h_1^2 + 2h_2^2 \right] \quad (B27)$$

$$B_{15} = \frac{4}{L_2} \left[(2D_1 + D_7 - D_8)Q_1 + (D_5 - D_6 - 2D_4)Q_2 - (D_5 + D_6)Q_3 + (D_7 + D_8)Q_4 \right. \\ \left. - (D_9 \sinh 2r)Q_5 - (D_{10} \sinh 2r)Q_6 - (D_9 \sin 2r)Q_7 - (D_{10} \sin 2r)Q_8 \right] \\ + \frac{4}{15M_3} \left[-20h_3 + 12h_4 + 18 \sinh 2r - 6 \sin 2r \right] \quad (B28)$$

$$\begin{aligned}
B_{16} = & \frac{4}{L_2} [(-D_5 + D_6 + 2D_4)Q_1 + (2D_1 + D_7 - D_8)Q_2 + (D_7 + D_8)Q_3 + (D_5 + D_6)Q_4 \\
& - (D_{10} \sinh 2r)Q_5 + (D_9 \sinh 2r)Q_6 - (D_{10} \sin 2r)Q_7 \\
& + (D_9 \sin 2r)Q_8] + \frac{4}{15M_3} [12h_3 - 20h_4 - 6 \sinh 2r + 18 \sin 2r]
\end{aligned} \tag{B29}$$

$$B_{17} = \frac{16h_3}{15M_3} \tag{B30}$$

$$B_{18} = \frac{16h_4}{15M_3} \tag{B31}$$

$$B_{19} = - \frac{8 \sinh 2r}{5M_3} \tag{B32}$$

$$B_{20} = - \frac{8 \sin 2r}{5M_3} \tag{B33}$$

$$\begin{aligned}
B_{21} = & \frac{4}{L_2} [(-2D_1 - D_7 + D_8)Q_2 + (D_5 - D_6 - 2D_4)Q_1 + (D_5 + D_6)Q_4 + (D_7 + D_8)Q_3 \\
& + (D_9 \sinh 2r)Q_7 + (D_{10} \sinh 2r)Q_8 - (D_9 \sin 2r)Q_5 \\
& - (D_{10} \sin 2r)Q_6] + \frac{4}{15M_3} [20h_4 + 12h_3 + 18 \sin 2r + 6 \sinh 2r]
\end{aligned} \tag{B34}$$

$$\begin{aligned}
B_{22} = & \frac{4}{L_2} [(D_5 - D_6 - 2D_4)Q_2 + (2D_1 + D_7 - D_8)Q_1 - (D_7 + D_8)Q_4 + (D_5 + D_6)Q_3 \\
& + (D_{10} \sinh 2r)Q_7 - (D_9 \sinh 2r)Q_8 - (D_{10} \sin 2r)Q_5 \\
& + (D_9 \sin 2r)Q_6] - \frac{4}{15M_3} [12h_4 + 20h_3 + 6 \sin 2r + 18 \sinh 2r]
\end{aligned} \tag{B35}$$

where

$$\begin{aligned}
 C_1 &= -\frac{2}{3} \sinh 2r \sin 2r - \frac{4}{3} \sinh r \sin r \\
 C_2 &= \frac{2}{3} \cosh 2r \cos 2r - 2 + \frac{4}{3} \cosh r \cos r \\
 C_3 &= -\frac{2}{5} \cos 2r - \frac{2}{5} \cosh 2r + \frac{4}{5} \cosh r \cos r \\
 C_4 &= -\frac{4}{5} \cos 2r + \frac{4}{5} \cosh 2r + \frac{4}{5} \sinh r \sin r \\
 C_5 &= \frac{2}{5} \sinh 2r \sin 2r + \frac{12}{5} \sinh r \sin r \\
 C_6 &= \frac{2}{5} \cosh 2r \cos 2r + 2 - \frac{12}{5} \cosh r \cos r
 \end{aligned}
 \tag{B36}$$

$$\begin{aligned}
 D_1 &= \cosh^2 r \cos^2 r \sinh r \sin r \\
 D_2 &= \sinh^3 r \sin^3 r \\
 D_3 &= \cosh^3 r \cos^3 r \\
 D_4 &= \sinh^2 r \sin^2 r \cosh r \cos r \\
 D_5 &= \cosh r \cos^3 r \sinh^2 r \\
 D_6 &= \cosh^3 r \cos r \sin^2 r \\
 D_7 &= \sinh^3 r \sin r \cos^2 r \\
 D_8 &= \cosh^2 r \sin^3 r \sinh r \\
 D_9 &= \sinh r \cos r \\
 D_{10} &= \cosh r \sin r
 \end{aligned}
 \tag{B37}$$

$$\left. \begin{aligned}
 E_1 &= \frac{2}{3} \cosh 2r \cos 2r + 2 - \frac{8}{3} \cosh r \cos r \\
 E_2 &= \frac{2}{3} \sinh 2r \sin 2r - \frac{8}{3} \sinh r \sin r \\
 E_3 &= -\frac{2}{5} \cos 2r + \frac{2}{5} \cosh 2r - \frac{8}{5} \sinh r \sin r \\
 E_4 &= -\frac{4}{5} \cos 2r - \frac{4}{5} \cosh 2r + \frac{8}{5} \cosh r \cos r \\
 E_5 &= -\frac{2}{5} \sinh 2r \sin 2r + \frac{8}{5} \sinh r \sin r \\
 E_6 &= -\frac{2}{5} \cosh 2r \cos 2r + 2 - \frac{8}{5} \cosh r \cos r
 \end{aligned} \right\} \quad (B38)$$

$$\left. \begin{aligned}
 h_1 &= \cosh r \cos r \\
 h_2 &= \sinh r \sin r \\
 h_3 &= \cosh r \sinh r (1 - 2 \cos^2 r) \\
 h_4 &= -\sin r \cos r (2 \cosh^2 r - 1)
 \end{aligned} \right\} \quad (B39)$$

$$\left. \begin{aligned}
 L_1 &= (\cosh^2 r + \cos^2 r - 1)^3 \\
 L_2 &= (\cosh^2 r - \cos^2 r)^2 (\cosh^2 r + \cos^2 r - 1)
 \end{aligned} \right\} \quad (B40)$$

$$\left. \begin{aligned}
 M_1 &= (\cosh^2 r + \cos^2 r - 1)^2 \\
 M_2 &= (\cosh^2 r - \cos^2 r)^2 \\
 M_3 &= (\cosh^2 r + \cos^2 r - 1) (\cosh^2 r - \cos^2 r) \\
 M_4 &= \cosh^2 r \sin^2 r \\
 M_5 &= \sin^2 r \cos^2 r
 \end{aligned} \right\} \quad (B41)$$

$$\begin{aligned}
 Q_1 &= \frac{2}{3} \cosh 2r \sin 2r - \frac{4}{3} \cosh r \sin r \\
 Q_2 &= \frac{2}{3} \sinh 2r \cos 2r - \frac{4}{3} \sinh r \cos r \\
 Q_3 &= \frac{2}{5} \sinh 2r \cos 2r - \frac{4}{5} \cosh r \sin r \\
 Q_4 &= -\frac{2}{5} \cosh 2r \sin 2r + \frac{4}{5} \sinh r \cos r \\
 Q_5 &= -\frac{2}{5} \sin 2r + \frac{6}{5} \sinh r \cos r - \frac{2}{5} \cosh r \sin r \\
 Q_6 &= -\frac{4}{5} \sin 2r + \frac{6}{5} \cosh r \sin r + \frac{2}{5} \sinh r \cos r \\
 Q_7 &= -\frac{2}{5} \sinh 2r + \frac{6}{5} \cosh r \sin r - \frac{2}{5} \sinh r \cos r \\
 Q_8 &= \frac{4}{5} \sinh 2r - \frac{6}{5} \sinh r \cos r - \frac{2}{5} \cosh r \sin r
 \end{aligned}
 \tag{B42}$$

Nusselt Number Constants

The constants appearing in equations (83) to (84) are given explicitly as

$$\begin{aligned}
 \Omega_1 &= (B_2 - B_1) \sinh r \cos r - (B_1 + B_2) \cosh r \sin r + 8(B_4 - B_3) \sinh 2r \cos 2r \\
 &\quad - 8(B_3 + B_4) \cosh 2r \sin 2r - 4B_5 (\sinh 2r - \sin 2r)
 \end{aligned}
 \tag{B43}$$

$$\begin{aligned}
 \Omega_2 &= (B_7 - B_6) \sinh r \cos r - (B_6 + B_7) \cosh r \sin r + 8(B_3 + B_4) \sinh 2r \cos 2r \\
 &\quad + 8(B_4 - B_3) \cosh 2r \sin 2r
 \end{aligned}
 \tag{B44}$$

$$\begin{aligned}
 \Omega_3 &= (B_9 - B_8) \sinh r \cos r - (B_8 + B_9) \cosh r \sin r + 8(B_{11} - B_{10}) \sinh 2r \cos 2r \\
 &\quad - 8(B_{10} + B_{11}) \cosh 2r \sin 2r + 4B_{12} (\sinh 2r + \sin 2r)
 \end{aligned}
 \tag{B45}$$

$$\begin{aligned}\Omega_4 = & (B_{14}-B_{13})\sinh r \cos r - (B_{13}+B_{14})\cosh r \sin r \\ & + 8(B_3-B_4)\sinh 2r \cos 2r + 8(B_3+B_4)\cosh 2r \sin 2r \\ & - 4B_5(\sinh 2r - \sin 2r)\end{aligned}\quad (B46)$$

$$\begin{aligned}\Omega_5 = & (B_{16}-B_{15})\cosh r \cos r - (B_{15}+B_{16})\sinh r \sin r \\ & + 8(B_{18}-B_{17})\cosh 2r \cos 2r - 8(B_{17}+B_{18})\sinh 2r \sin 2r \\ & - 4B_{19} \cos 2r + 4B_{20} \cosh 2r\end{aligned}\quad (B47)$$

$$\begin{aligned}\Omega_6 = & (B_{22}-B_{21})\cosh r \cos r - (B_{21}+B_{22})\sinh r \sin r \\ & + 8(B_{17}+B_{18})\cosh 2r \cos 2r - 8(B_{17}-B_{18})\sinh 2r \sin 2r \\ & - 4B_{20} \cos 2r - 4B_{19} \cosh 2r\end{aligned}\quad (B48)$$

REFERENCES

1. Ostrach, Simon: Laminar Natural-Convection Flow and Heat Transfer of Fluids with and without Heat Sources in Channels with Constant Wall Temperatures. NACA TN 2863, 1952.
2. Lighthill, M. J.: Theoretical Considerations on Free Convection in Tubes. F.M. 1758, Aero. Res. Council, July 21, 1952.
3. Martinelli, R. C., and Boelter, L. M. K.: The Analytical Prediction of Superposed Free and Forced Viscous Convection in a Vertical Pipe. Univ. Calif. Press (Berkeley and Los Angeles), 1942.
4. Goldstein, S.: Modern Developments in Fluid Dynamics. Vol. II. Clarendon Press (Oxford), 1938, pp. 622-623.
5. Nusselt, Wilhelm: Die Abhängigkeit der Wärmeübergangszahl von der Rohrlänge. Z.V.D.I., Bd. 54, 1910, pp. 1154-1158.
6. Eagle, A. E., and Ferguson, R. M.: On the Coefficient of Heat Transfer from the Internal Surface of Tube Walls. Proc. Roy. Soc. (London), ser. A, vol. 127, 1930, pp. 540-566.
7. Hamilton, D. C., Poppendiek, H. F., and Palmer, L. D.: Theoretical and Experimental Analyses of Natural Convection within Fluids in which Heat is being Generated - Part I: Heat Transfer from a Fluid in Laminar Flow to Two Parallel Plane Bounding Walls: A Simplified Velocity Distribution was Postulated. CF 51-12-70, Oak Ridge Nat. Lab., Dec. 18, 1951.

8. Bosworth, R. C. L.: Heat Transfer Phenomena. John Wiley & Sons, Inc., 1952.
9. Eckert, E. R. G., and Jackson, Thomas W.: Analysis of Turbulent Free-Convection Boundary Layer on Flat Plate. NACA Rep. 1015, 1951. (Supersedes NACA TN 2207.)
10. Ostrach, Simon: An Analysis of Laminar Free-Convection Flow and Heat Transfer about a Flat Plate Parallel to the Direction of the Generating Body Force. NACA Rep. 1111, 1953. (Supersedes NACA TN 2635.)
11. Ostroumov, G. A.: Mathematical Theory of the Steady Heat Transfer in a Circular Vertical Hole with Superposition of Forced and Free Laminar Convection. Jour. Tech. Phys., vol. XX, no. 6, 1950.
12. Ostrach, Simon: New Aspects of Natural-Convection Heat Transfer. Trans. A.S.M.E., vol. 75, no. 7, Oct. 1953, pp. 1287-1290.
13. Havemann, H. A.: Critical Cooling. Mech. Eng., Bangalore (India), no. 1, Oct. 1950, pp. 16-25.
14. Prandtl, Ludwig: "Führer durch die Strömungslehre. Friedr. Vieweg und Sohn (Braunschweig), 1949.
15. de Graaf, J. G. A., and van der Held, E. F. M.: The Relation Between the Heat Transfer and the Convection Phenomena in Enclosed Plane Air Layers. Appl. Sci. Res., sec. A, vol. 3, no. 6, 1953, pp. 393-409.
16. Watzinger, A., und Johnson, Dag G.: Wärmeübertragung von Wasser an Rohrwand bei senkrechter Strömung in Übergangsgebiet zwischen laminarer und turbulenter Strömung. Forsch. Geb. Ing. - Wes., Bd. 10, Heft 4, Juli/Aug. 1939, pp. 182-196.

TABLE I. - ZEROth ORDER UNIVERSAL FUNCTIONS

(a) $Ra = 10$

η	v_{00}	v_{01}	v_{02}	v_{01}''
0	0.8821	0	-0.3571	0
.1	.8835	-.01293	-.3536	.07812
.2	.8876	-.02504	-.3431	.1563
.3	.8946	-.03570	-.3256	.2347
.4	.9041	-.04387	-.3011	.3132
.5	.9159	-.04902	-.2694	.3921
.6	.9298	-.05028	-.2304	.4713
.7	.9457	-.04676	-.1842	.5507
.8	.9628	-.03771	-.1304	.6304
.9	.9811	-.02237	-.06901	.7104
1.0	1.0	0	0	.7906

(b) $Ra = 10^2$

η	v_{00}	v_{01}	v_{02}	v_{01}''
0	0.36002	0	-0.59713	0
.1	.36748	-.03828	-.59260	.2220
.2	.38973	-.07435	-.57890	.4463
.3	.42644	-.10594	-.55537	.6753
.4	.47700	-.13079	-.52119	.9108
.5	.54057	-.14651	-.4751	1.1545
.6	.61597	-.15069	-.4154	1.4073
.7	.70173	-.14079	-.3402	1.6694
.8	.79597	-.11419	-.2476	1.9402
.9	.89632	-.06818	-.1350	2.2180
1.0	1.000	0	0	2.5000

(c) $Ra = 1600$

η	v_{00}	v_{01}	v_{02}	v_{01}''
0	-0.1342	0	-0.1672	0
.1	-.1258	-.06668	-.1735	.09850
.2	-.09985	-.1322	-.1929	.2639
.3	-.05462	-.1951	-.2217	.5616
.4	-.01291	-.2522	-.2558	1.053
.5	.1061	-.2986	-.2886	1.798
.6	.2279	-.3266	-.3105	2.840
.7	.3806	-.3258	-.3092	4.209
.8	.5638	-.2828	-.2696	5.897
.9	.7745	-.1807	-.1736	7.862
1.0	1.000	0	0	10.00

(d) $Ra = 10^4$

η	v_{00}	v_{01}	v_{02}	v_{01}''
0	-0.053806	0	0.022326	0
.1	-.056456	-.012229	.015544	-.6621
.2	-.062696	-.031015	-.0054315	-1.2444
.3	-.067254	-.062081	-.042058	-1.6264
.4	-.060949	-.10908	-.095256	-1.6120
.5	-.030510	-.17164	-.16322	-.9074
.6	.040867	-.24238	-.23796	.8741
.7	.17153	-.30309	-.30121	4.1660
.8	.37653	-.32059	-.32004	9.3285
.9	.65964	-.24313	-.24306	16.449
1.0	1.0000	0	0	25.000

TABLE II. - FIRST ORDER UNIVERSAL FUNCTIONS

(a) $Re = 10$

η	v_{10}	v_{11}	v_{12}	v_{13}	v_{14}	v_{15}	v_{10}^*	v_{11}^*	v_{12}^*	v_{13}^*	v_{14}^*	v_{15}^*
0	0.3382×10^{-2}	0.87802×10^{-2}	0.2979×10^{-2}	2.8555×10^{-2}	0	0	-0.7217×10^{-2}	-2.0733×10^{-2}	-0.7480×10^{-2}	-8.0109×10^{-2}	0	0
.1	.3349	.86789	.2941	2.8228	.000305 $\times 10^{-2}$	0	-.7214	-2.0763	-.7352	-8.0180	.01315 $\times 10^{-2}$.02082 $\times 10^{-2}$
.2	.3243	.8555	.2829	2.7310	.000750	0	-.7224	-2.0811	-.6985	-8.0368	.02077	.02774
.3	.3084	.8400	.265	2.5824	.00158	0	-.7225	-2.0793	-.6431	-8.0375	.01862	.00892
.4	.2818	.8104	.241	2.3705	.00252	0	-.7110	-2.0550	-.5729	-8.0382	.00359	-.04130
.5	.2497	.7179	.210	2.0994	.00349	0	-.6835	-1.8866	-.5008	-8.0152	-.02256	-.1211
.6	.2111	.6058	.175	1.7892	.00427	0	-.6535	-1.6494	-.4287	-8.4802	-.06512	-.2188
.7	.1641	.4752	.135	1.5083	.0044	0	-.6443	-1.6143	-.3495	-8.8219	-.0859	-.3077
.8	.1140	.3279	.092	.9578	.0039	0	-.4157	-1.2474	-.2872	-3.7918	-.1001	-.3454
.9	.0599	.1863	.047	.4897	.00184	0	-.2351	-.7206	-.1617	-2.2500	-.0785	-.2720
1.0	0	0	0	0	0	0	0	0	0	0	0	0

(b) $Re = 10^2$

η	v_{10}	v_{11}	v_{12}	v_{13}	v_{14}	v_{15}	v_{10}^*	v_{11}^*	v_{12}^*	v_{13}^*	v_{14}^*	v_{15}^*
0	5.2952×10^{-3}	4.8174×10^{-3}	1.4380×10^{-3}	4.001×10^{-3}	0	0	-8.7782×10^{-3}	-8.1120×10^{-3}	-3.647×10^{-3}	-8.998×10^{-3}	0	0
.1	5.2475	4.4767	1.4178	3.988	.0083 $\times 10^{-3}$	0	-8.838	-8.8515	-3.574	-7.123	.2174 $\times 10^{-3}$.0326 $\times 10^{-3}$
.2	5.0886	4.3533	1.3640	3.859	.0147	0	-8.8448	-8.8448	-3.565	-7.478	.3466	.0101
.3	4.8461	4.1435	1.2769	3.678	.0256	0	-11.009	-9.2161	-3.058	-8.017	.3156	-.1155
.4	4.483	3.8412	1.1581	3.416	.0411	0	-11.832	-9.845	-2.895	-8.851	.0872	-.3735
.5	4.005	3.4408	1.0142	3.068	.0668	0	-11.988	-10.341	-2.339	-9.237	-.8281	-.7851
.6	3.408	2.9370	.8458	2.627	.1136	0	-11.824	-10.480	-2.025	-9.585	-.8887	-1.2448
.7	2.690	2.3292	.6573	2.093	.0721	0	-10.829	-9.898	-1.7570	-9.323	-1.3814	-1.6973
.8	1.868	1.6258	.4814	1.465	.0623	0	-8.695	-8.251	-1.4711	-8.087	-1.5884	-1.9064
.9	.9585	.8387	.2308	.757	.0372	0	-5.156	-5.113	-.9939	-5.249	-1.2800	-1.6218
1.0	0	0	0	0	0	0	0	0	0	0	0	0

(c) $Re = 1800$

η	v_{10}	v_{11}	v_{12}	v_{13}	v_{14}	v_{15}	v_{10}^*	v_{11}^*	v_{12}^*	v_{13}^*	v_{14}^*	v_{15}^*
0	82.749×10^{-8}	-2.0180×10^{-8}	40.700×10^{-8}	11.235×10^{-8}	0	0	348.90×10^{-8}	77.722×10^{-8}	-84.076×10^{-8}	35.570×10^{-8}	0	0
.1	84.445	-1.8235	40.281	11.408	-.24869 $\times 10^{-8}$	0	308.62	78.511	-82.11	30.080	48.385 $\times 10^{-8}$	-35.433 $\times 10^{-8}$
.2	89.138	-.44978	59.048	11.876	-.02481	0	183.05	78.279	-76.47	15.119	85.675	-86.556
.3	95.594	1.5000	57.047	12.488	1.0383	0	-15.879	89.322	-88.28	-5.878	100.23	-90.303
.4	101.85	4.1285	54.384	13.040	3.0736	0	-277.74	41.088	-80.85	-28.696	80.06	-108.28
.5	103.27	7.1424	51.086	13.506	5.6736	0	-578.37	-18.74	-59.95	-83.098	18.46	-118.38
.6	102.96	9.9368	27.183	13.038	8.7691	0	-863.27	-115.55	-75.30	-82.580	-94.62	-134.88
.7	92.071	11.555	22.484	11.625	10.731	0	-1082.8	-236.32	-114.09	-122.82	-232.49	-183.40
.8	70.729	10.627	16.852	9.5925	10.388	0	-1069.4	-334.63	-188.2	-188.88	-344.06	-189.69
.9	38.954	6.851	9.185	5.593	6.673	0	-756.1	-310.67	-182.8	-175.30	-323.14	-194.82
1.0	0	0	0	0	0	0	0	0	0	0	0	0

(d) $Re = 10^4$

η	v_{10}	v_{11}	v_{12}	v_{13}	v_{14}	v_{15}	v_{10}^*	v_{11}^*	v_{12}^*	v_{13}^*	v_{14}^*	v_{15}^*
0	-17.545×10^{-8}	-15.785×10^{-8}	23.394×10^{-8}	29.095×10^{-8}	0	0	33.587×10^{-8}	-1.4532×10^{-8}	9.0287×10^{-8}	10.167×10^{-8}	0	0
.1	-.7187	-18.488	27.857	34.104	-8.7581 $\times 10^{-8}$	0	34.055	-.94889	8.5848	9.2564	1.0689 $\times 10^{-8}$.92580 $\times 10^{-8}$
.2	50.139	-18.005	40.585	48.215	-12.402	0	45.714	.71188	6.3265	6.5237	2.6739	.7884
.3	135.18	-18.712	59.810	60.713	-15.288	0	71.109	3.7608	2.6995	2.1226	5.2898	-1.1384
.4	250.38	-15.359	81.018	91.262	-12.825	0	94.230	7.9142	-2.1724	-3.256	8.7500	-4.618
.5	385.58	-4.5475	100.35	110.51	-1.8890	0	112.70	-5.8575	-7.189	-8.373	11.562	-8.533
.6	511.01	17.250	112.61	121.58	20.431	0	122.73	-52.880	-11.090	-11.929	8.825	-11.800
.7	584.12	47.011	113.78	120.73	50.144	0	121.16	-114.13	-14.588	-14.906	-6.091	-14.530
.8	542.90	70.018	100.09	104.70	78.54	0	104.74	-185.23	-21.897	-21.62	-34.418	-21.386
.9	341.82	59.52	84.35	86.62	80.92	0	68.51	-152.08	-31.50	-31.36	-55.410	-31.28
1.0	0	0	0	0	0	0	0	0	0	0	0	0

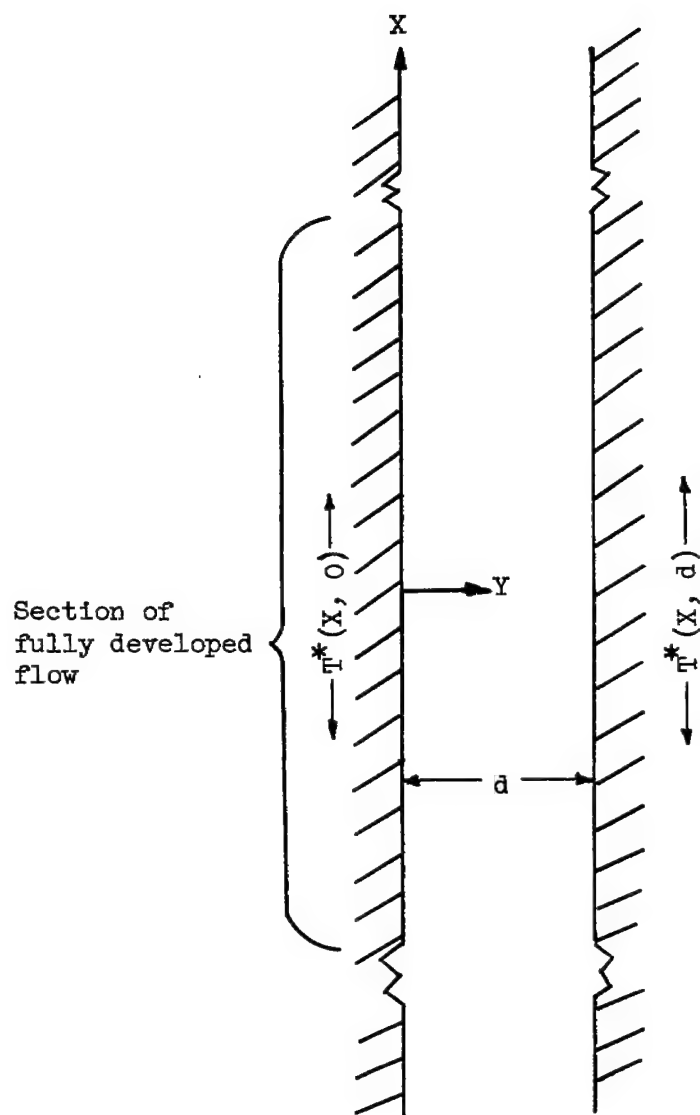


Figure 1. - Schematic sketch of configuration considered.

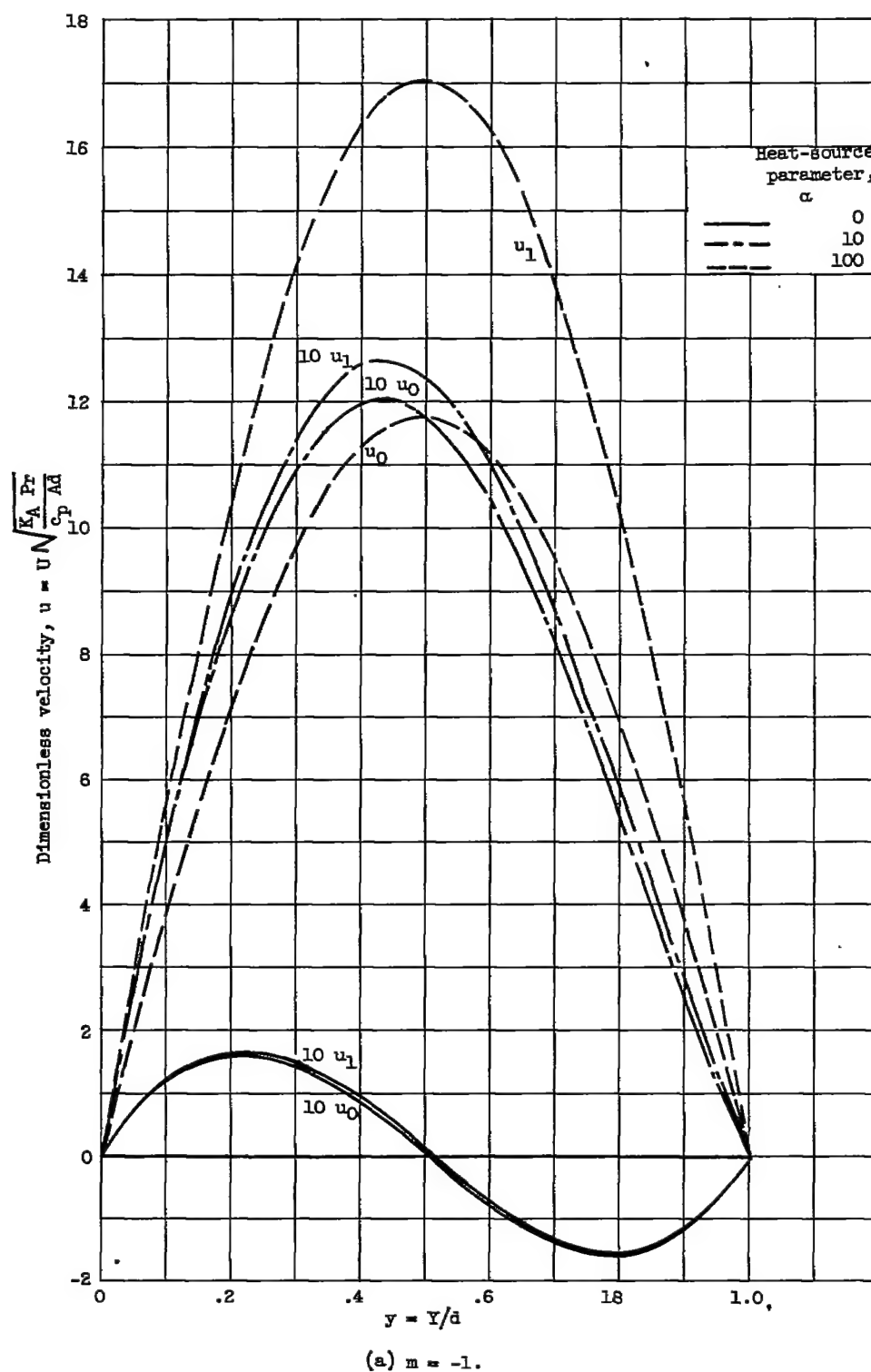


Figure 2. - Dimensionless velocity distributions for various heat-source parameters with $Ra = 10$, $K_A = 10$, $C = -1$.

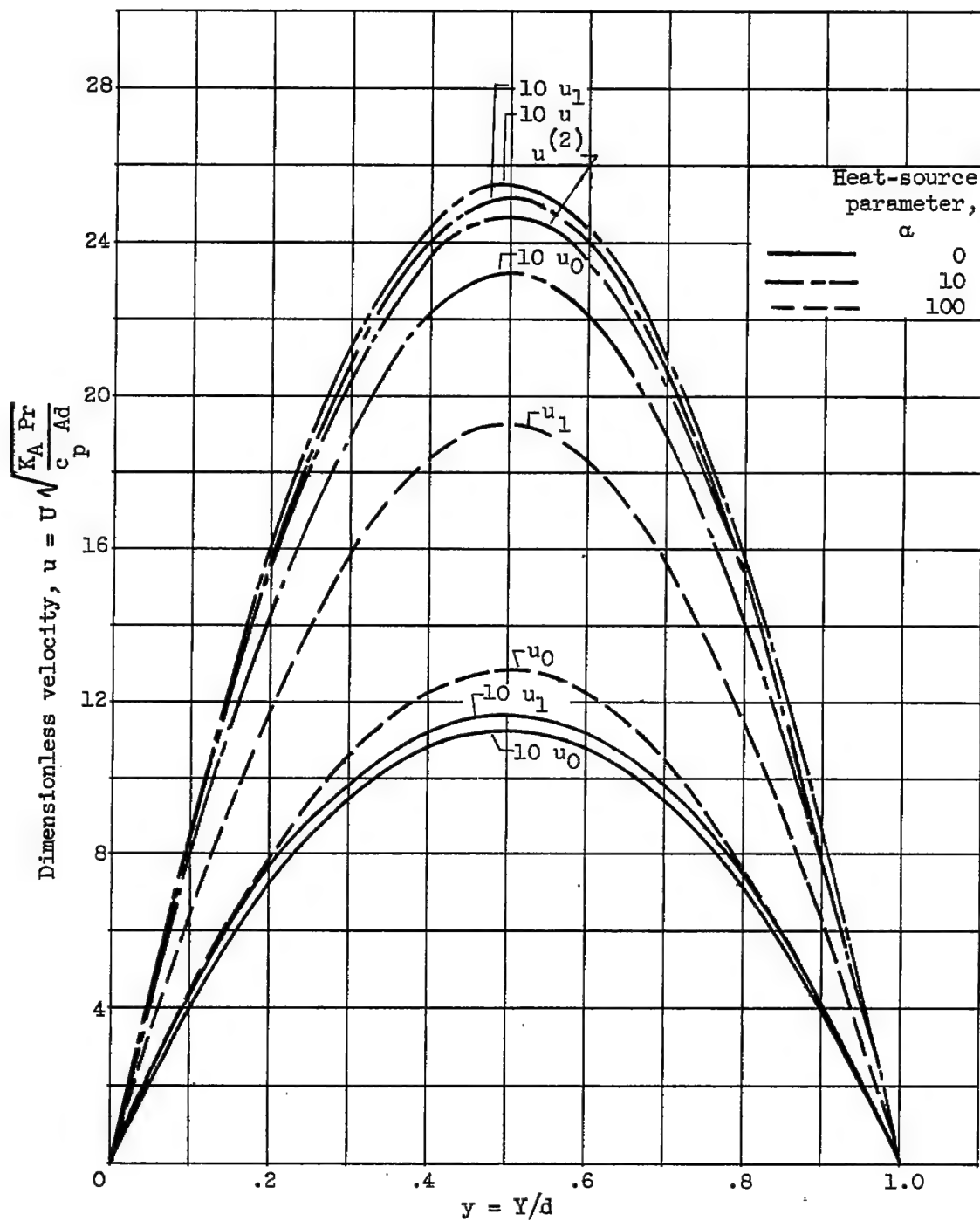
(b) $m = 1$.

Figure 2. - Continued. Dimensionless velocity distributions for various heat-source parameters with $Ra = 10$, $K_A = 10$, $C = -1$.

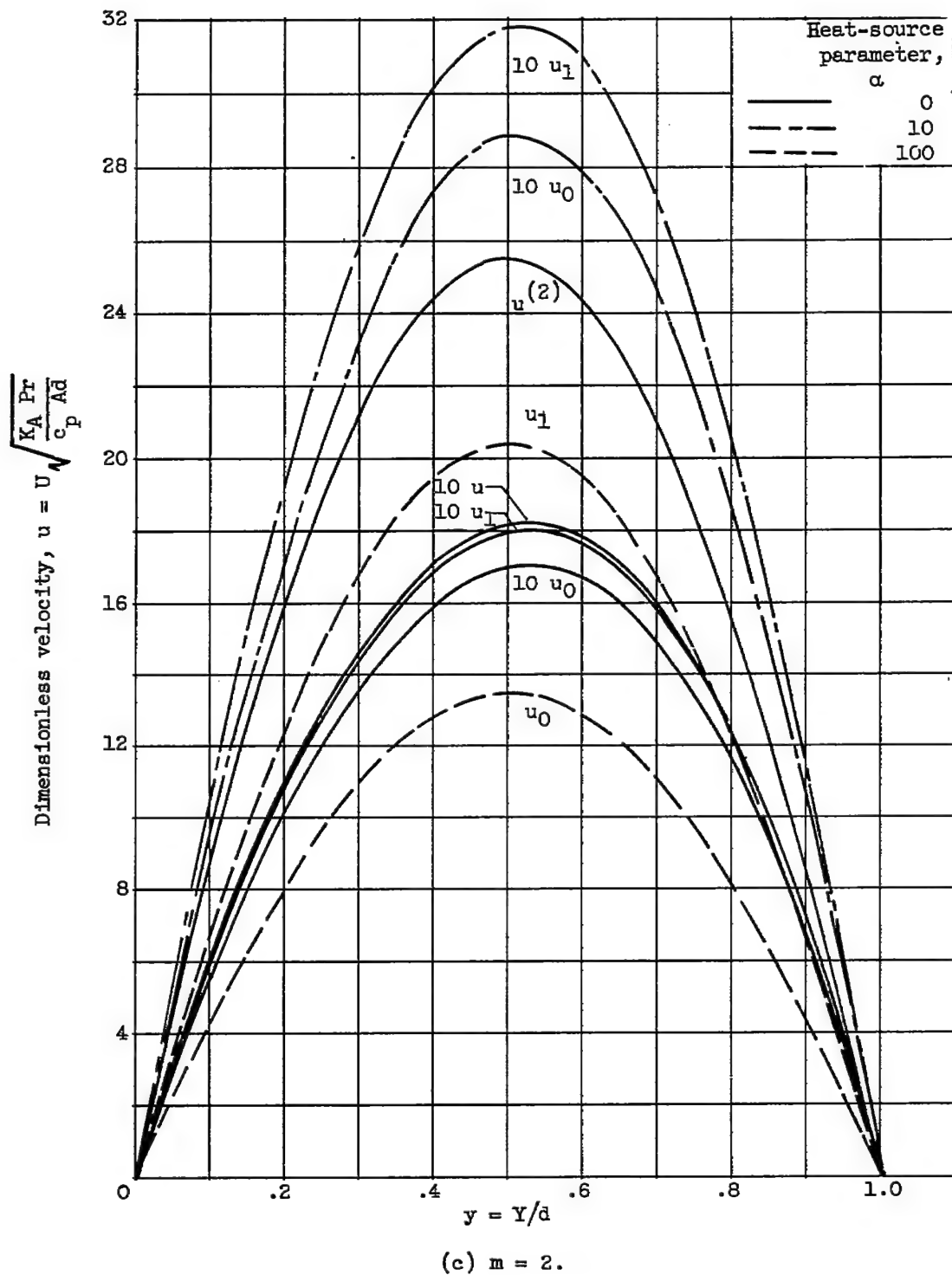


Figure 2. - Concluded. Dimensionless velocity distributions for various heat-source parameters with $Ra = 10$, $K_A = 10$, $C = -1$.

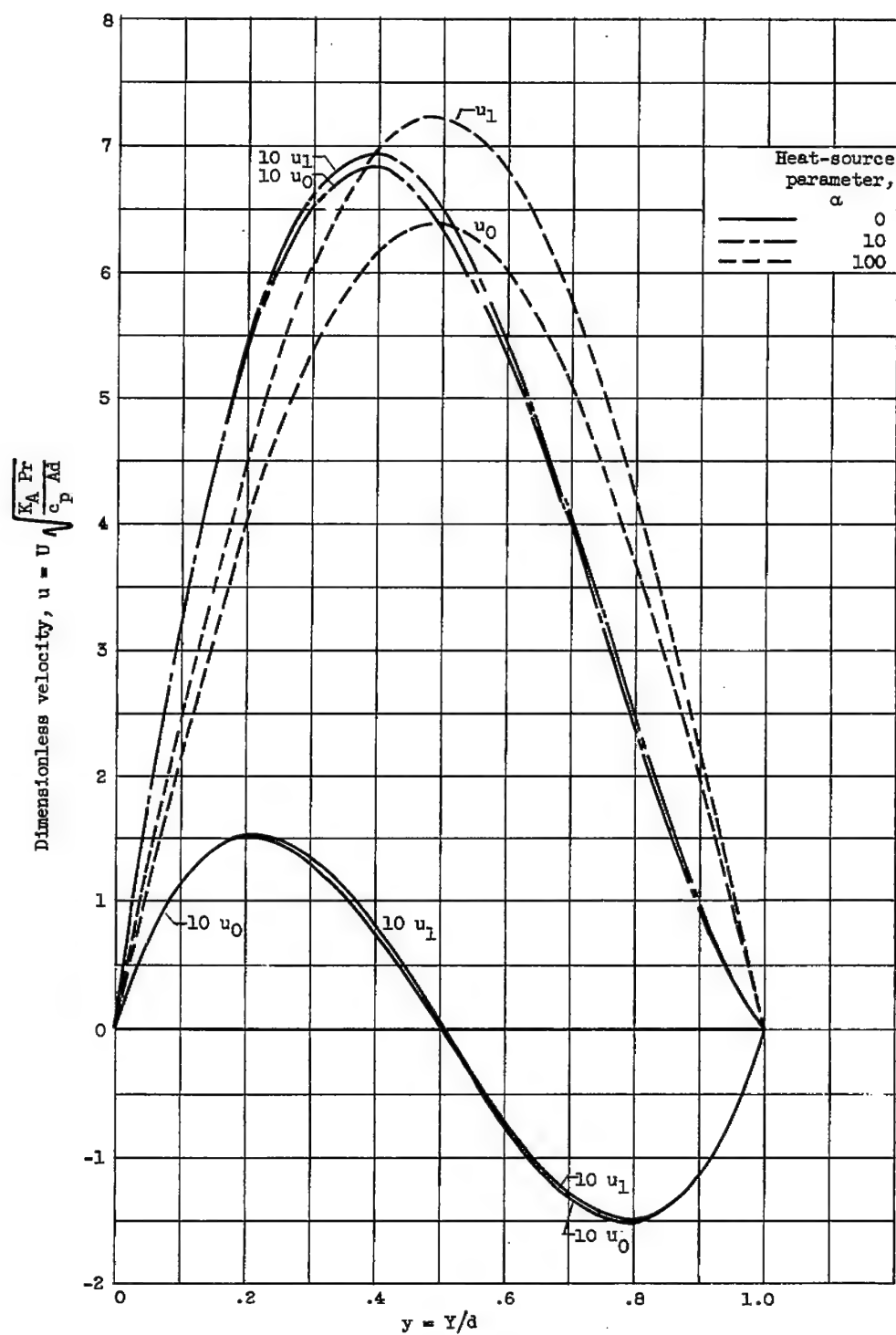
(a) $m = -1$.

Figure 3. - Dimensionless velocity distributions for various heat-source parameters with $Ra = 10^6$, $K_A = 10$, $C = -1$.

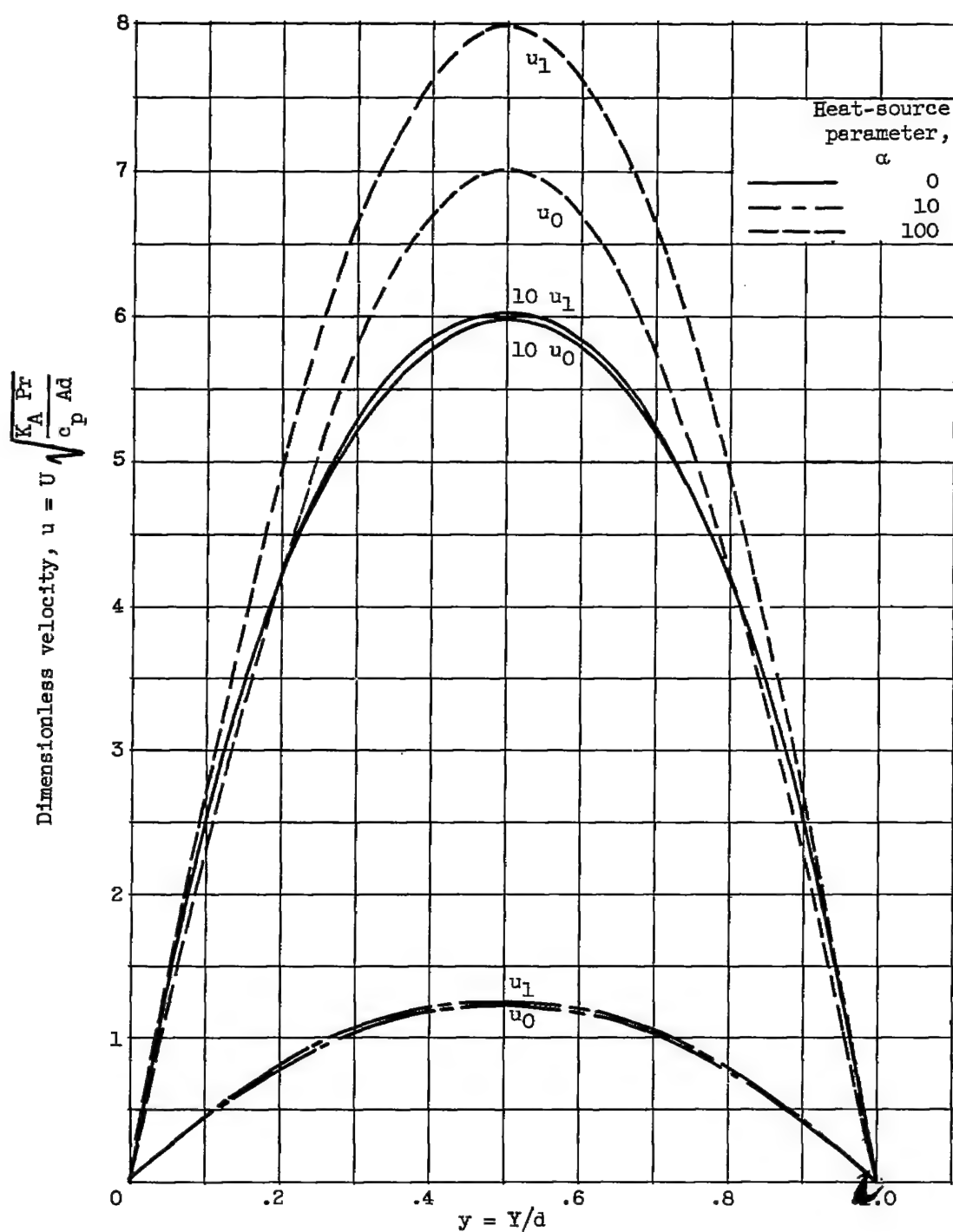


Figure 3. - Continued. Dimensionless velocity distributions for various heat-source parameters with $Ra = 10^4$, $K_A = 10$, $C = -1$.

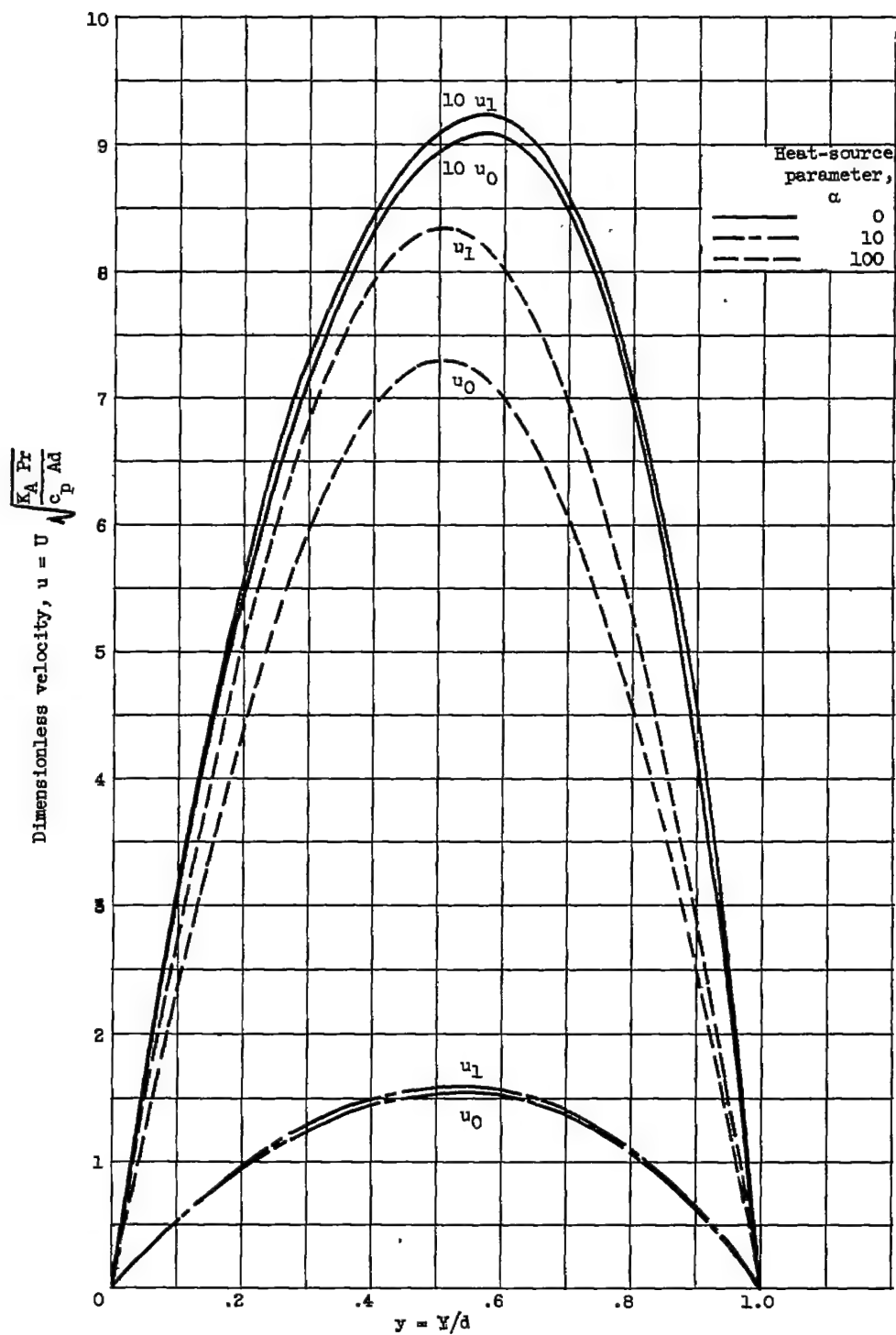
(c) $n = 2$.

Figure 3. - Concluded. Dimensionless velocity distributions for various heat-source parameters with $Ra = 10^2$, $K_A = 10$, $C = -1$.

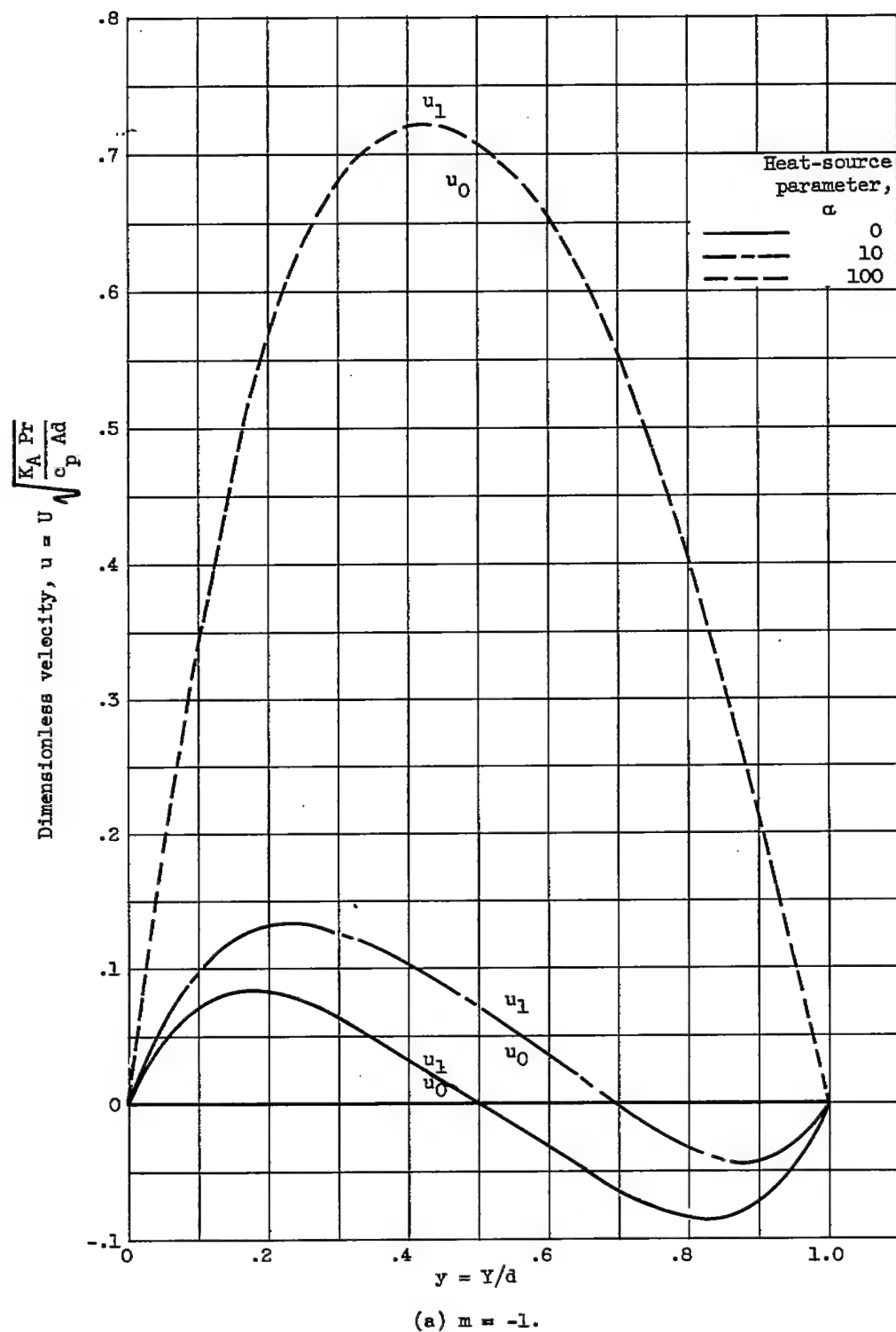


Figure 4. - Dimensionless velocity distributions for various heat-source parameters with $Ra = 1600$, $K_A = 10$, $C = -1$.

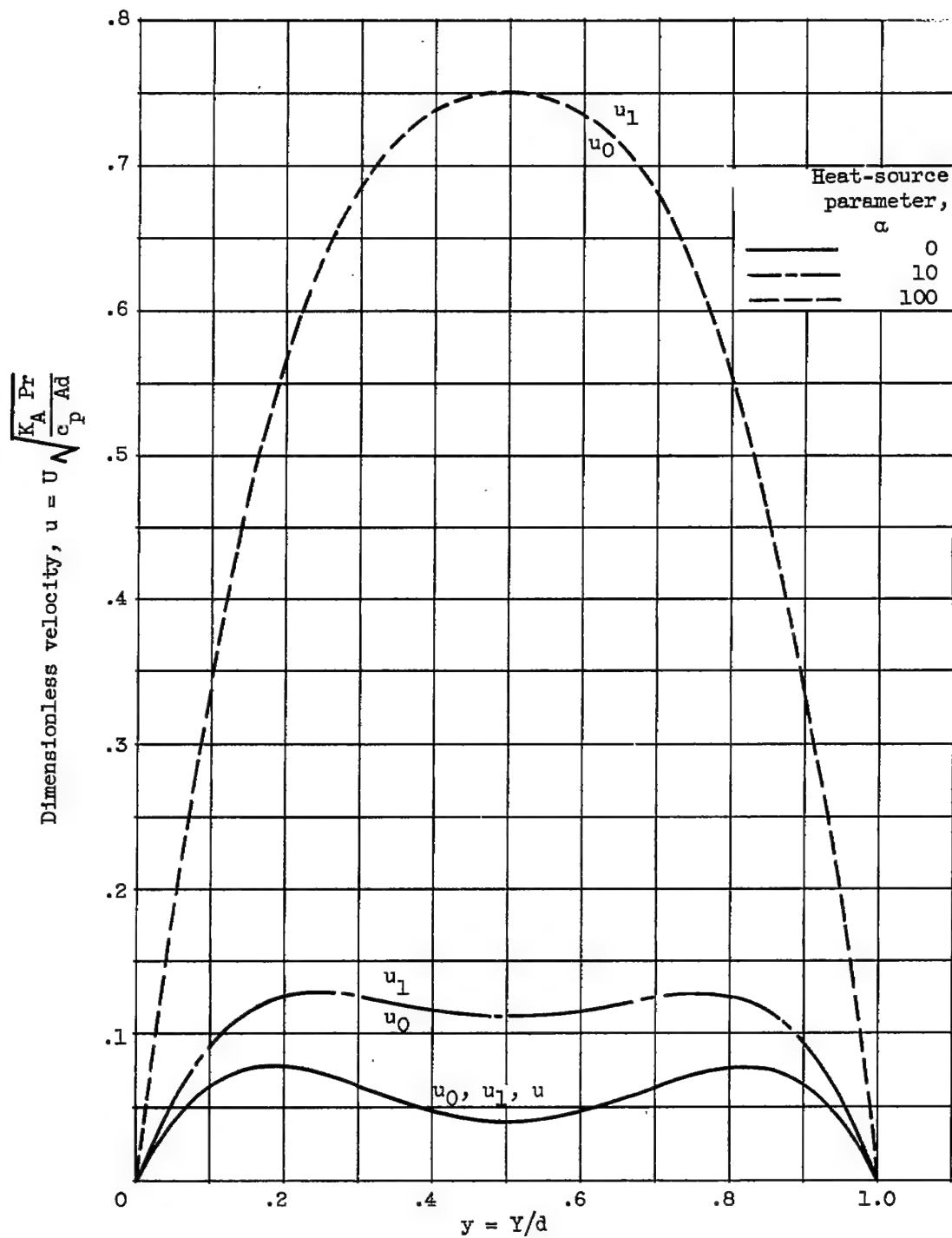
(b) $m = 1$.

Figure 4. - Continued. Dimensionless velocity distributions for various heat-source parameters with $Ra = 1600$, $K_A = 10$, $C = -1$.

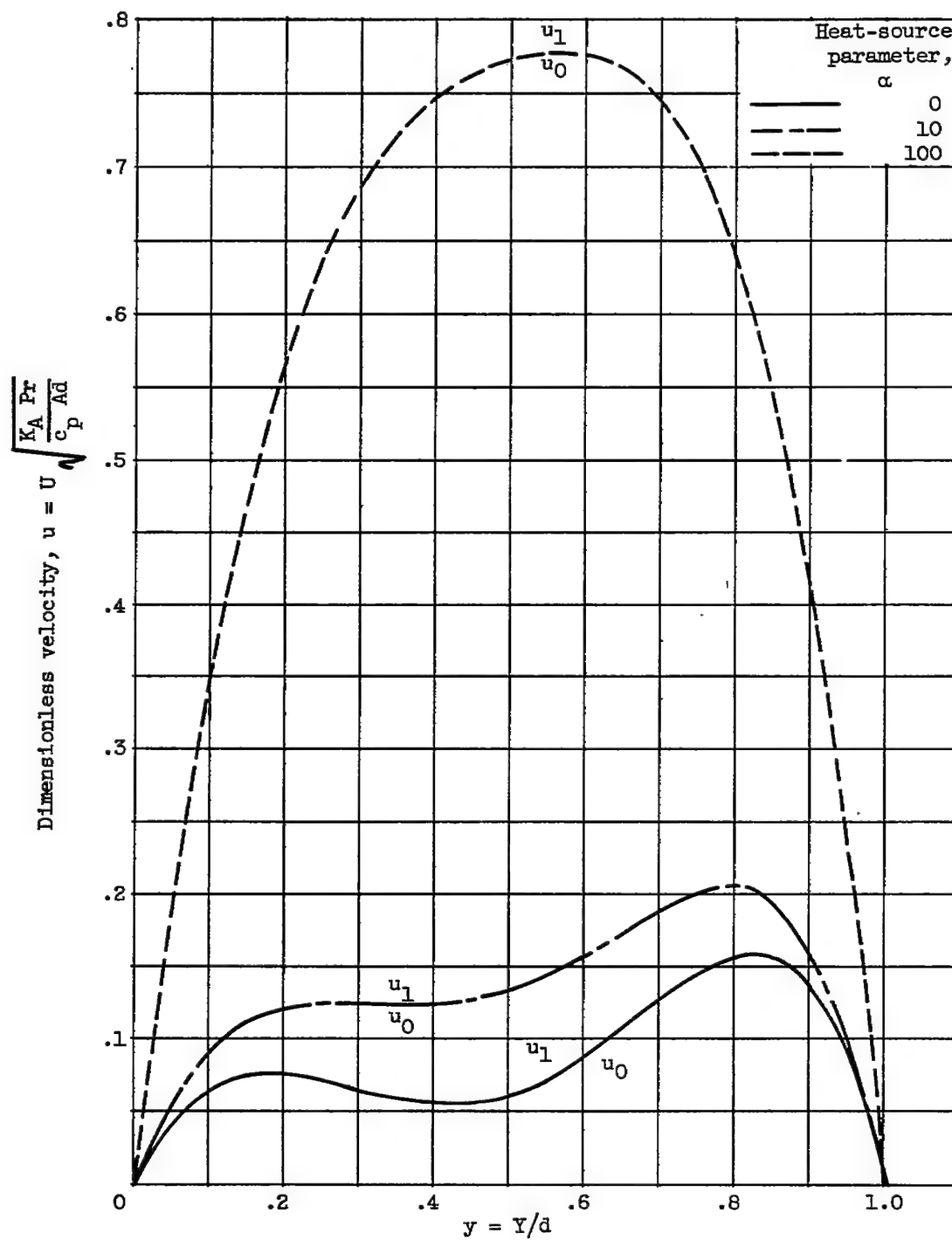
(c) $m = 2$.

Figure 4. - Concluded. Dimensionless velocity distributions for various heat-source parameters with $Ra = 1600$, $K_A = 10$, $C = -1$.

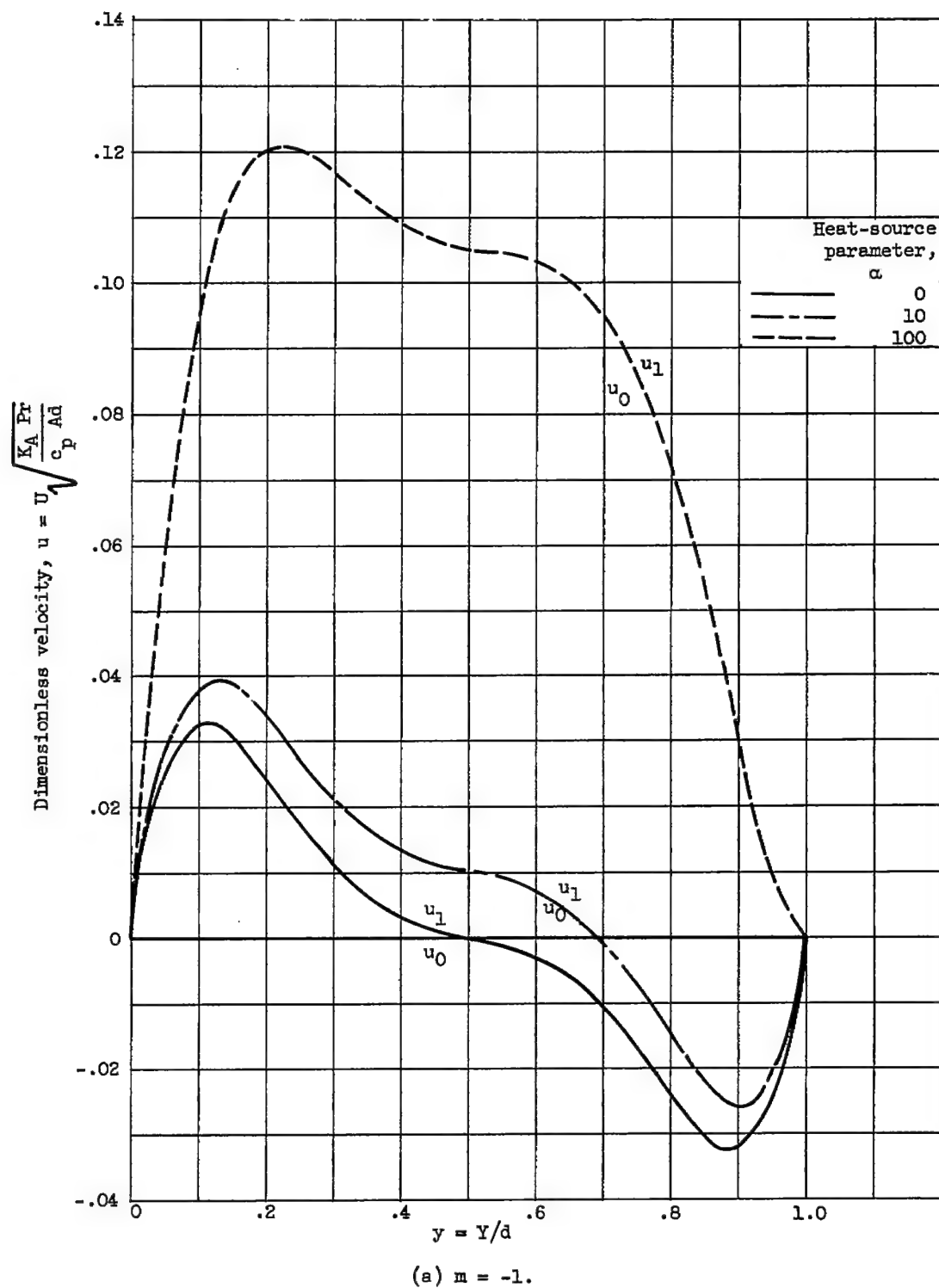


Figure 5. - Dimensionless velocity distributions for various heat-source parameters with $Ra = 10^4$, $K_A = 10$, $C = -1$.

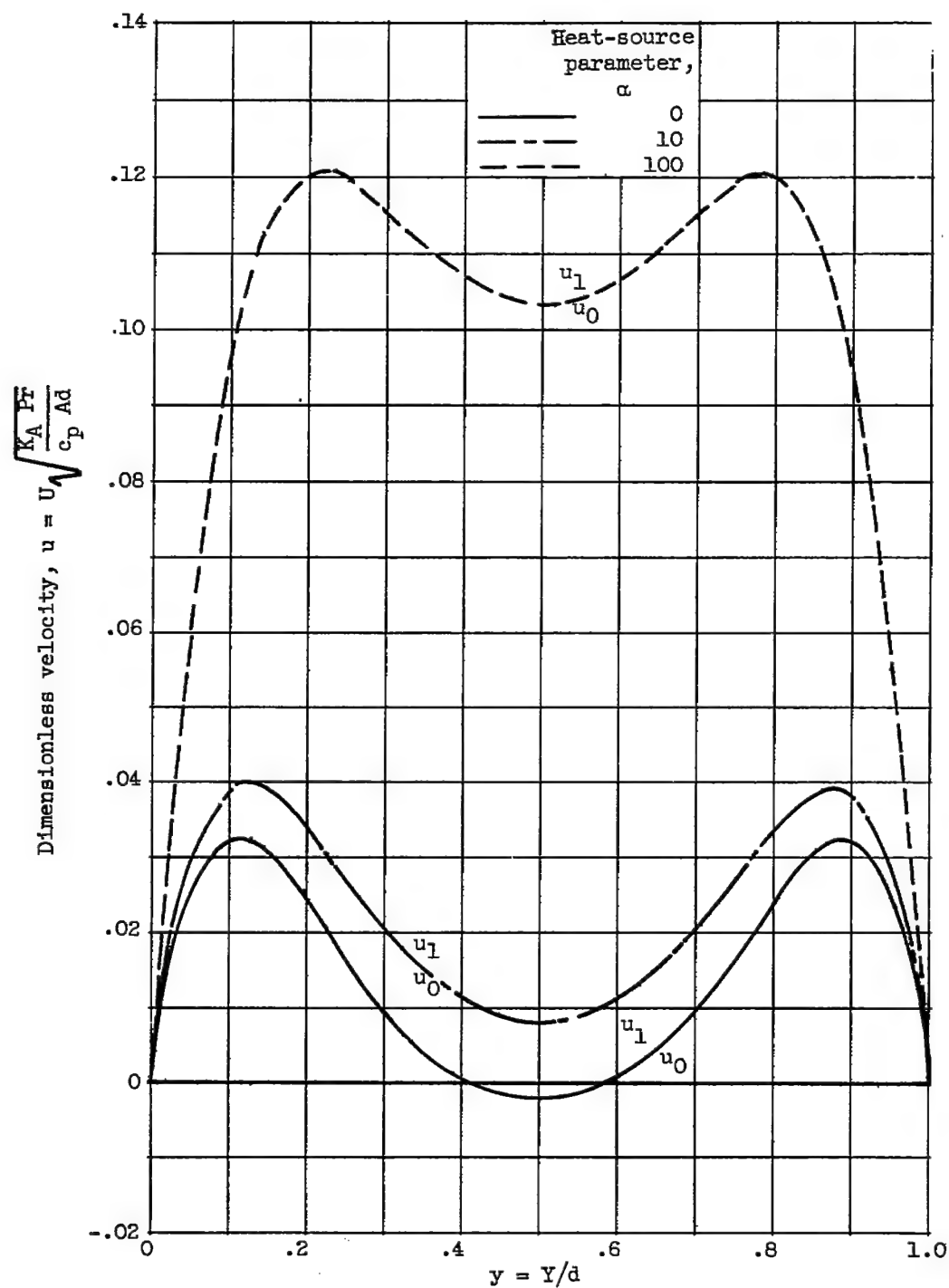
(b) $m = 1$.

Figure 5. - Continued. Dimensionless velocity distributions for various heat-source parameters with $Ra = 10^4$, $K_A = 10$, $C = -1$.

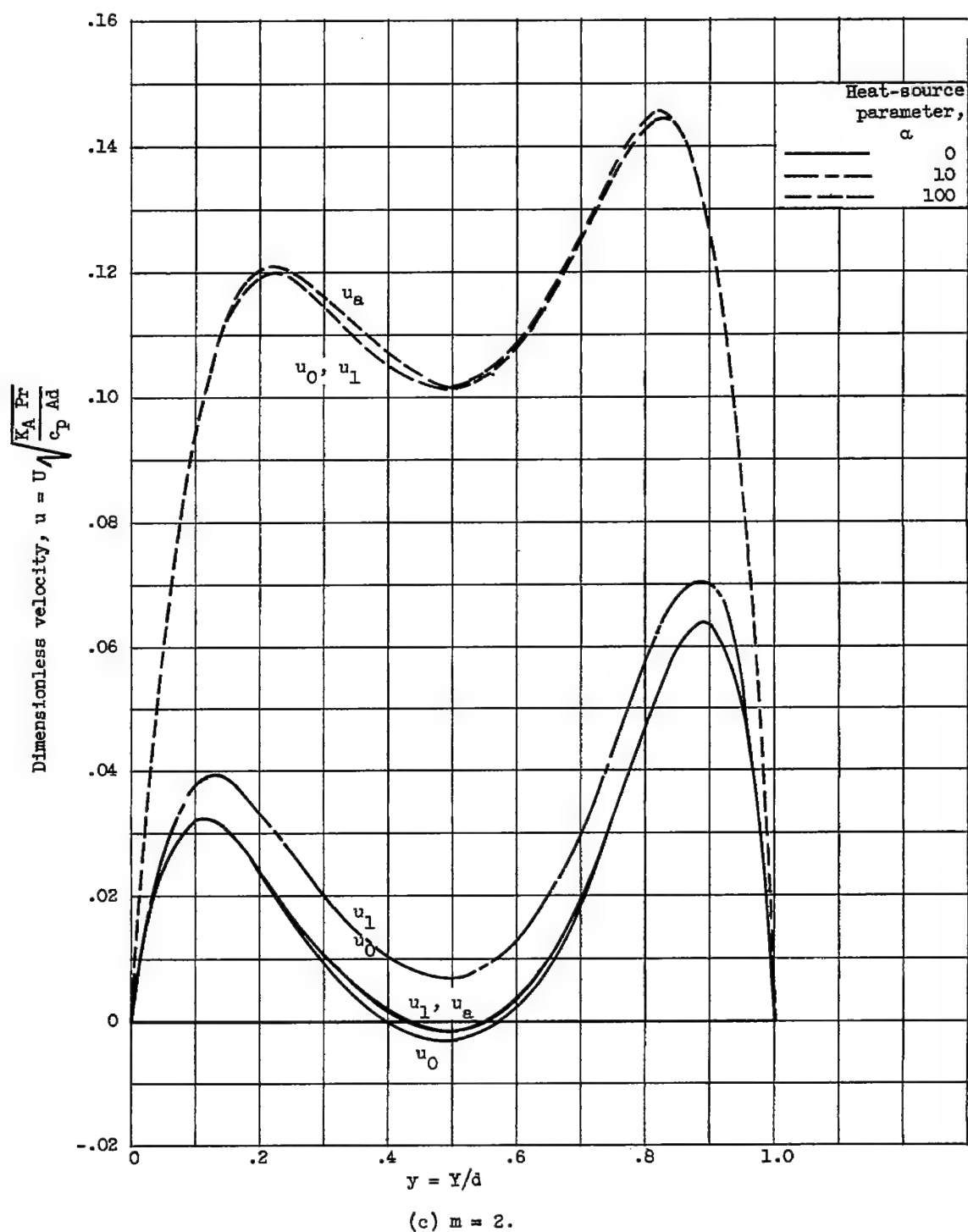


Figure 5. - Concluded. Dimensionless velocity distributions for various heat-source parameters with $Ra = 10^4$, $K_A = 10$, $C = -1$.

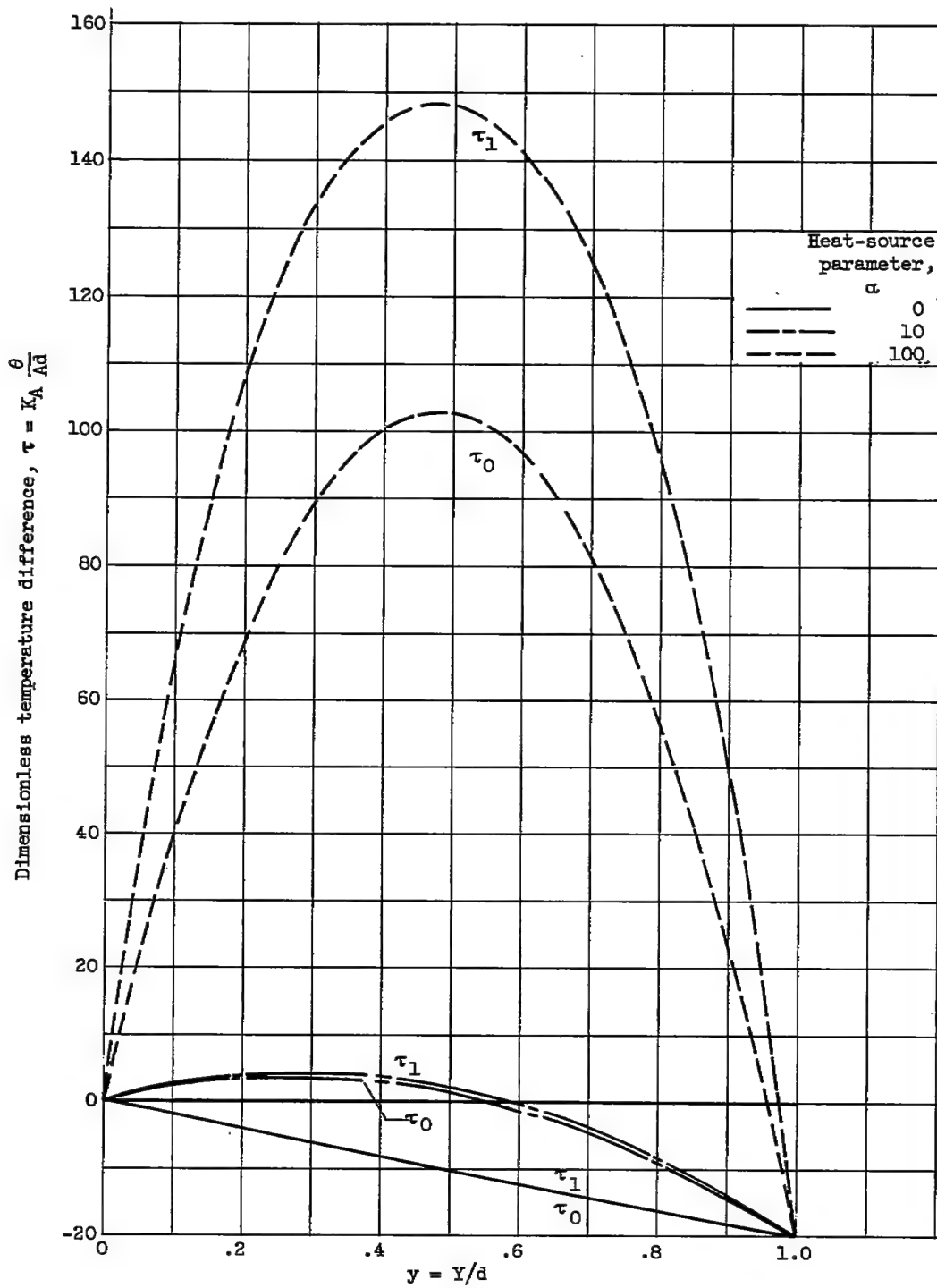
(a) $m = -1$.

Figure 6. - Dimensionless temperature distributions for various heat-source parameters with $Re = 10$, $K_A = 10$, $C = -1$.

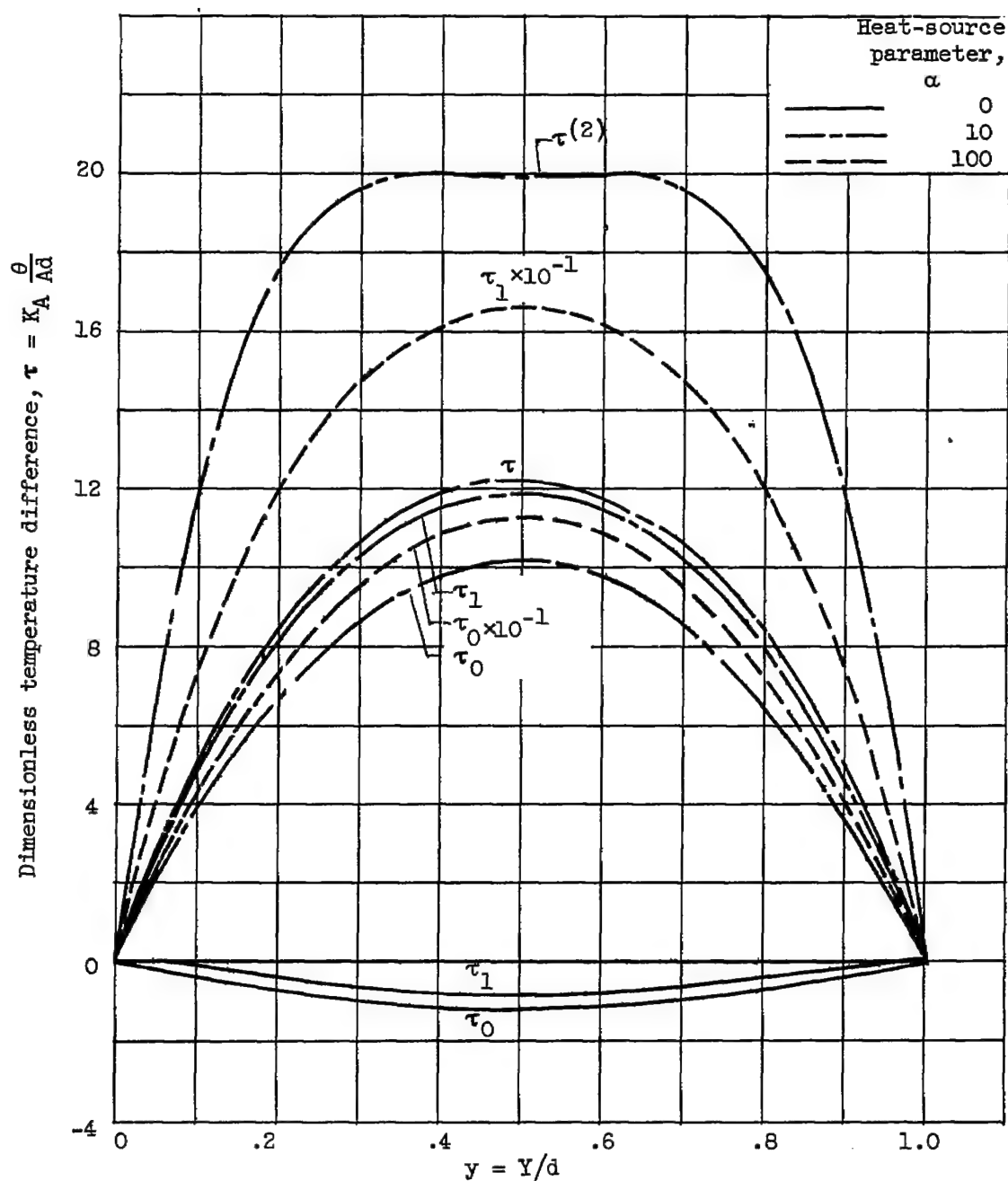
(b) $m = 1$.

Figure 6 . - Continued. Dimensionless temperature distributions for various heat-source parameters with $Ra = 10$, $K_A = 10$, $C = -1$.

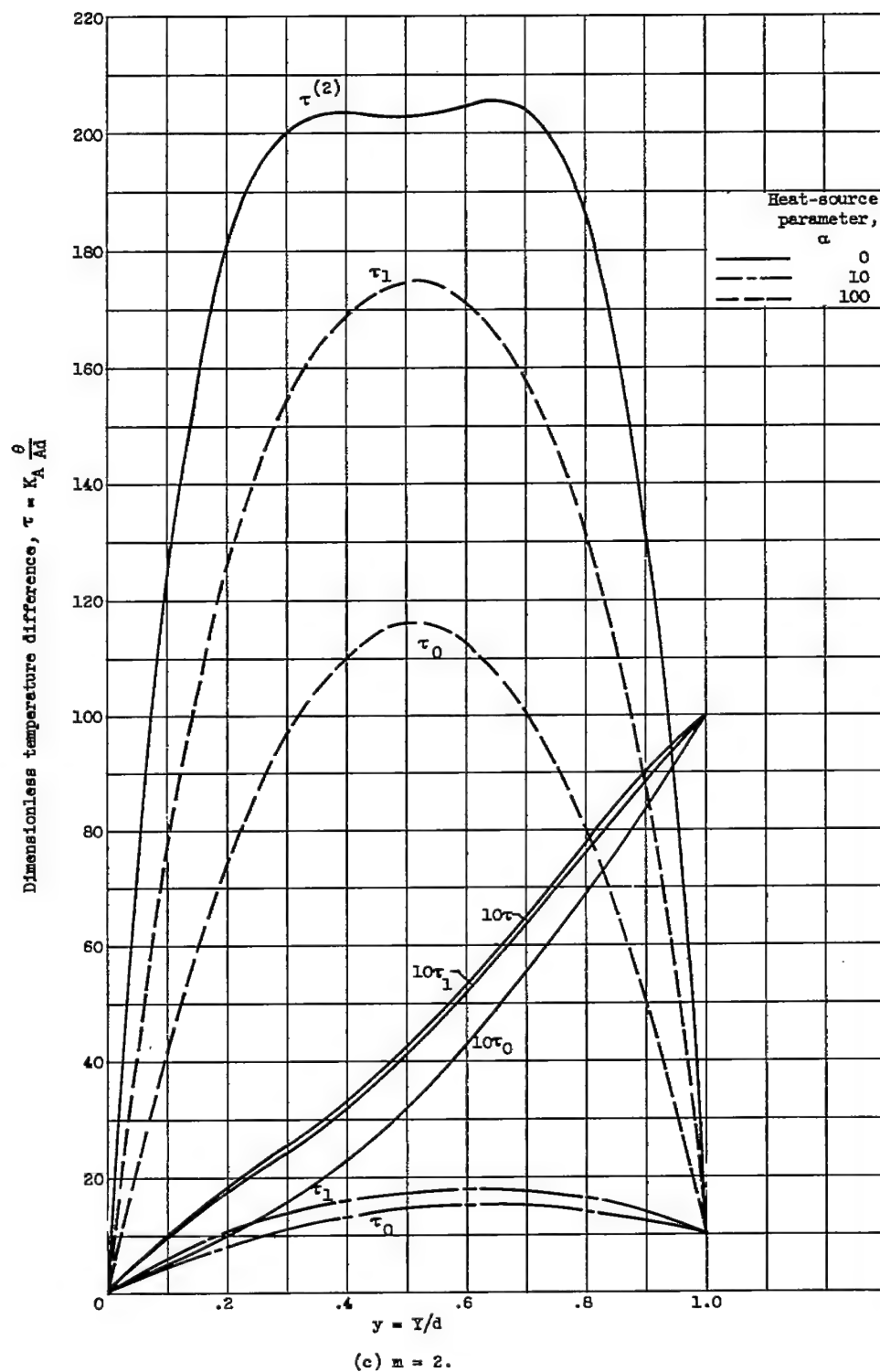


Figure 6. - Concluded. Dimensionless temperature distributions for various heat-source parameters with $Ra = 10$, $K_A = 10$, $C = -1$.

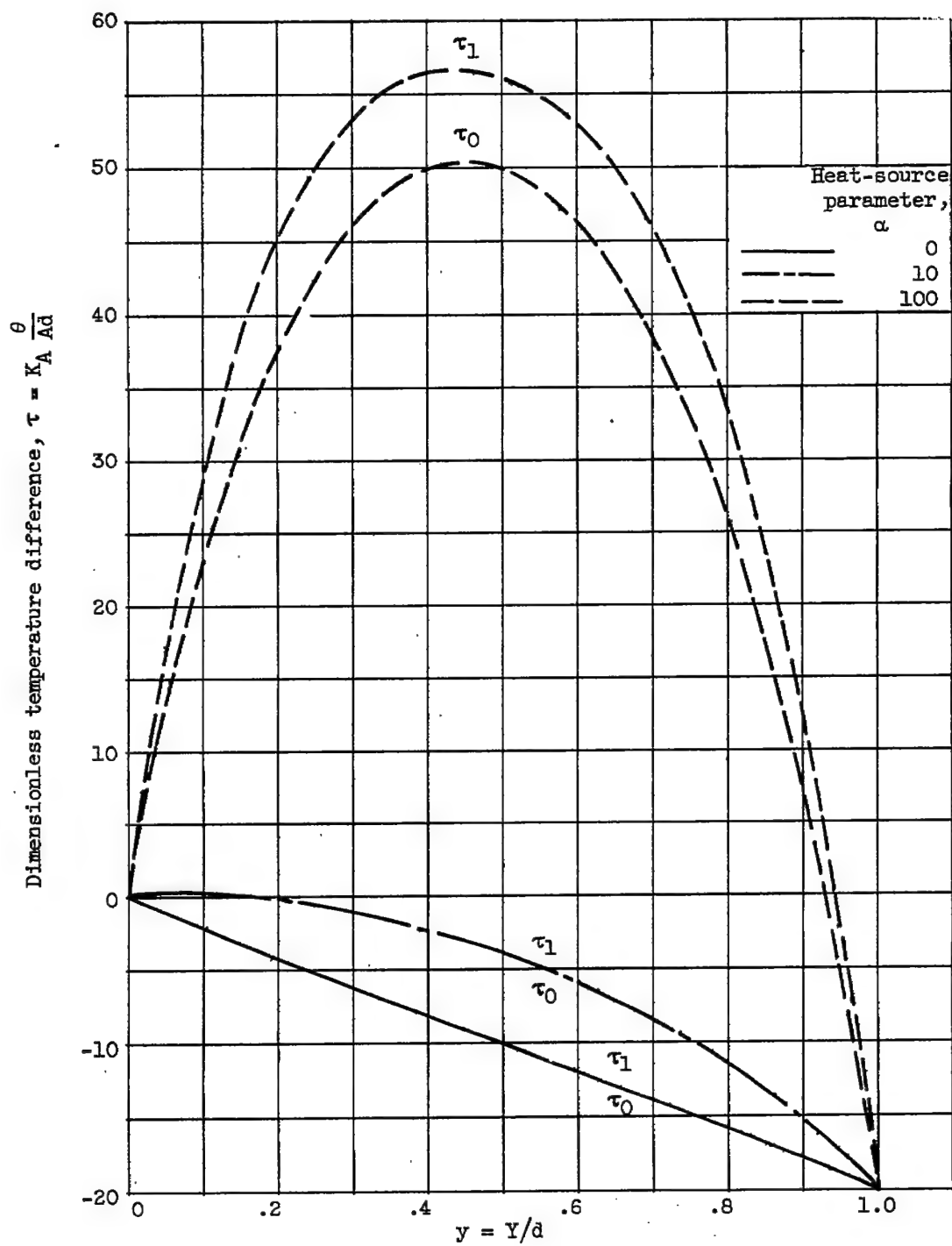
(a) $m = -1$.

Figure 7. - Dimensionless temperature distributions for various heat-source parameters with $Ra = 10^2$, $K_A = 10$, $C = -1$.

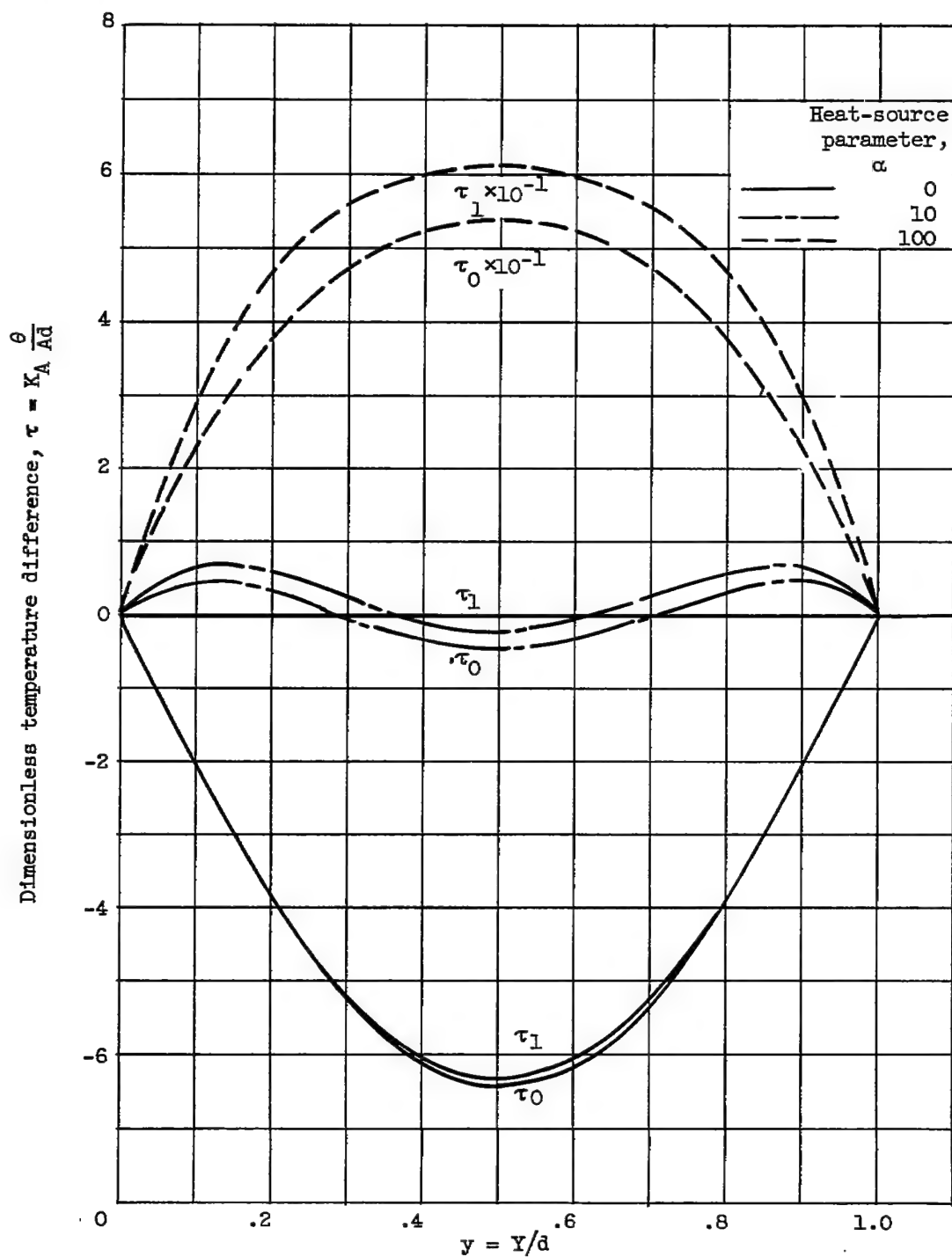


Figure 7. - Continued. Dimensionless temperature distributions for various heat-source parameters with $Ra = 10^2$, $K_A = 10$, $C = -1$.

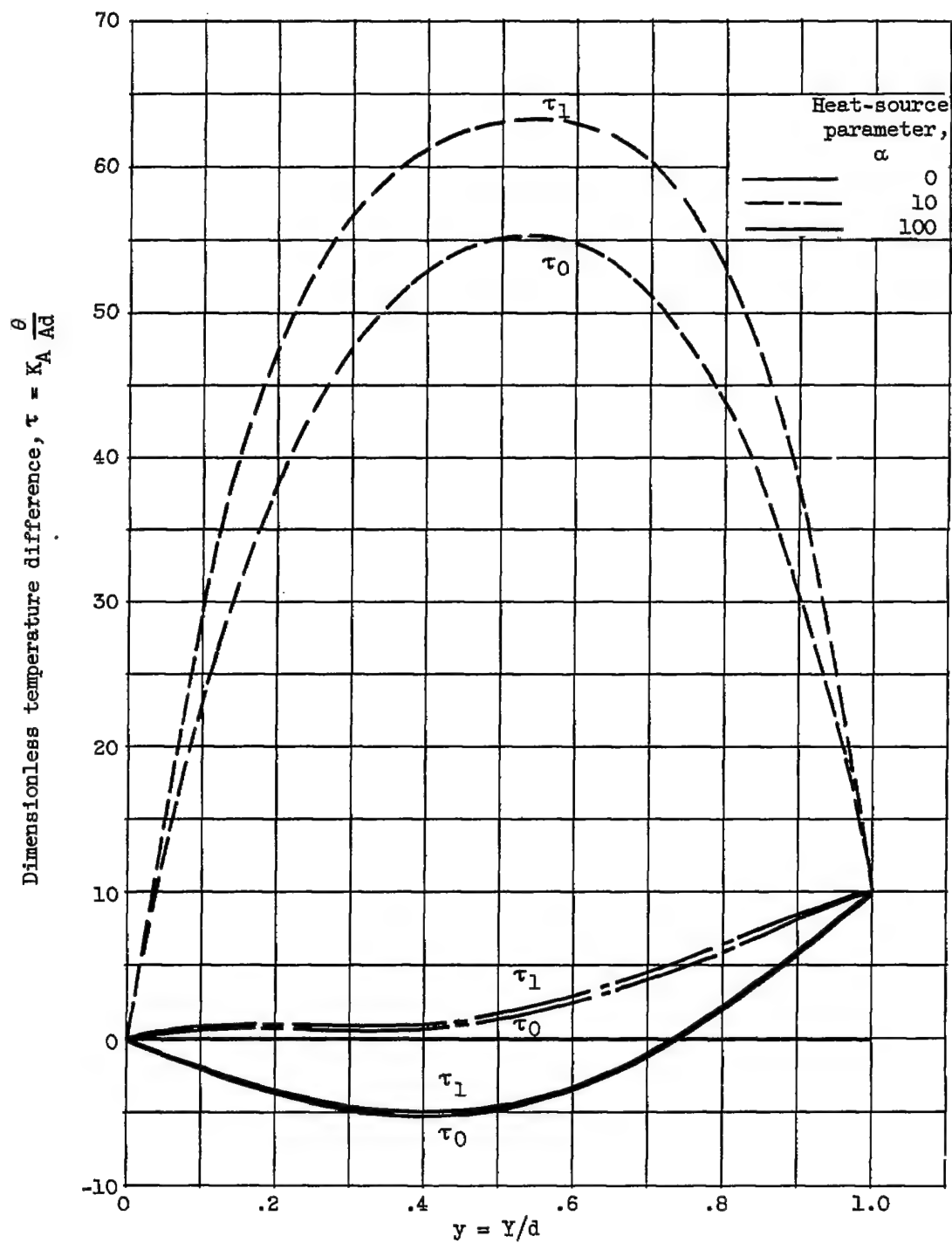
(c) $m = 2$.

Figure 7. - Concluded. Dimensionless temperature distributions for various heat-source parameters with $Ra = 10^2$, $K_A = 10$, $C = -1$.

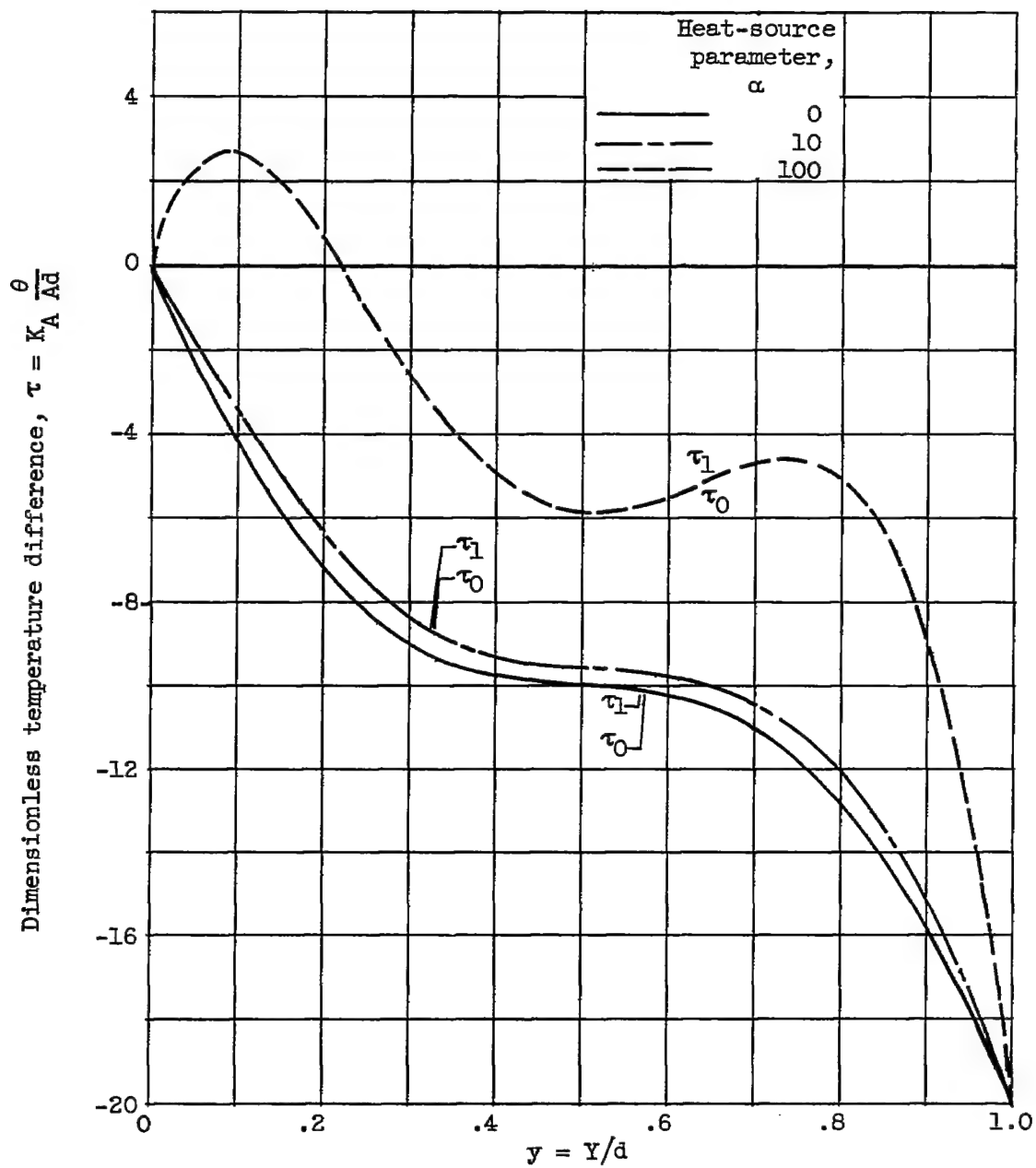
(a) $m = -1$.

Figure 8. - Dimensionless temperature distributions for various heat-source parameters with $Ra = 1600$, $K_A = 10$, $C = -1$.

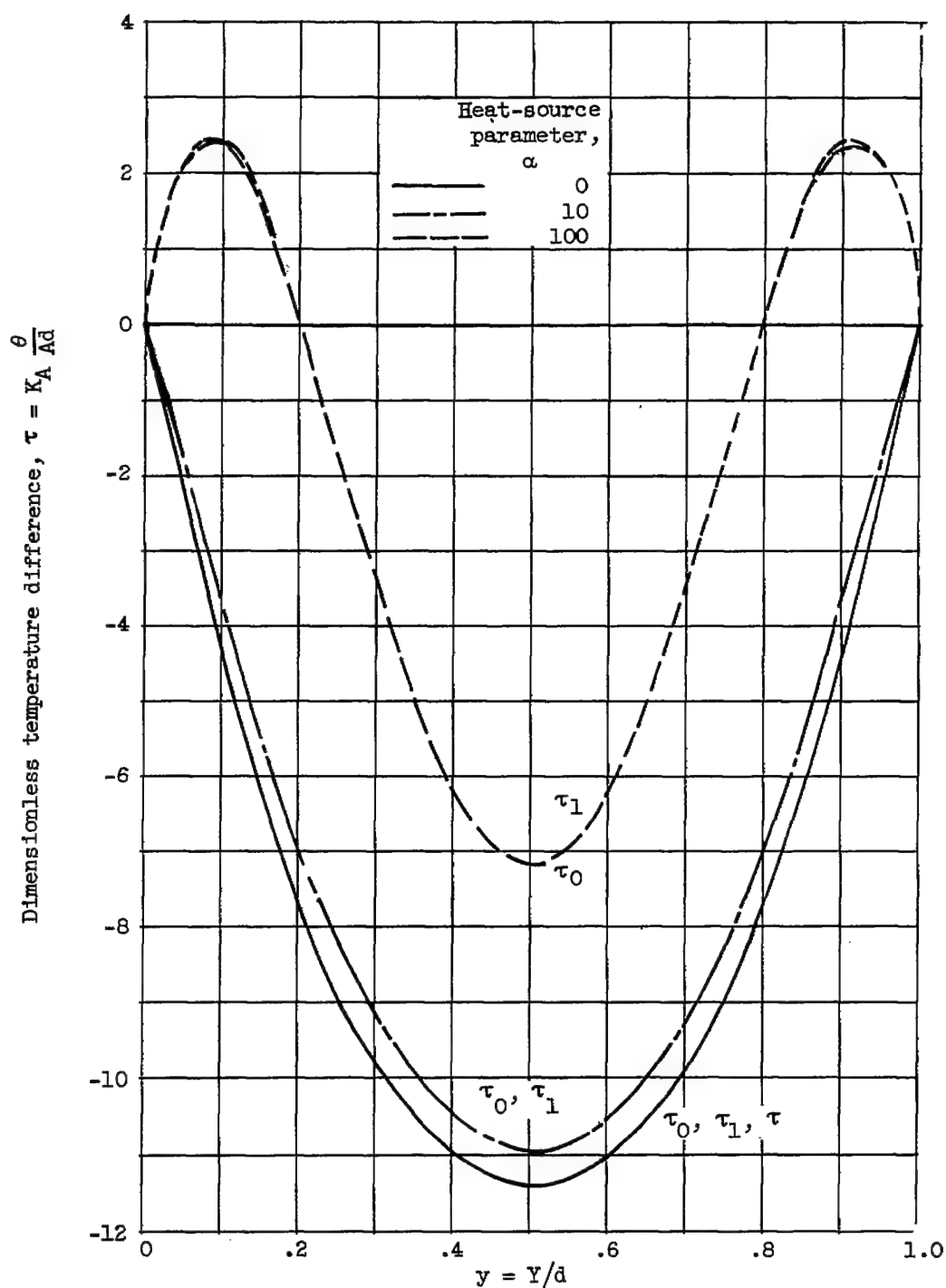
(b) $m = 1$.

Figure 8. - Continued. Dimensionless temperature distributions for various heat-source parameters with $Ra = 1600$, $K_A = 10$, $C = -1$.

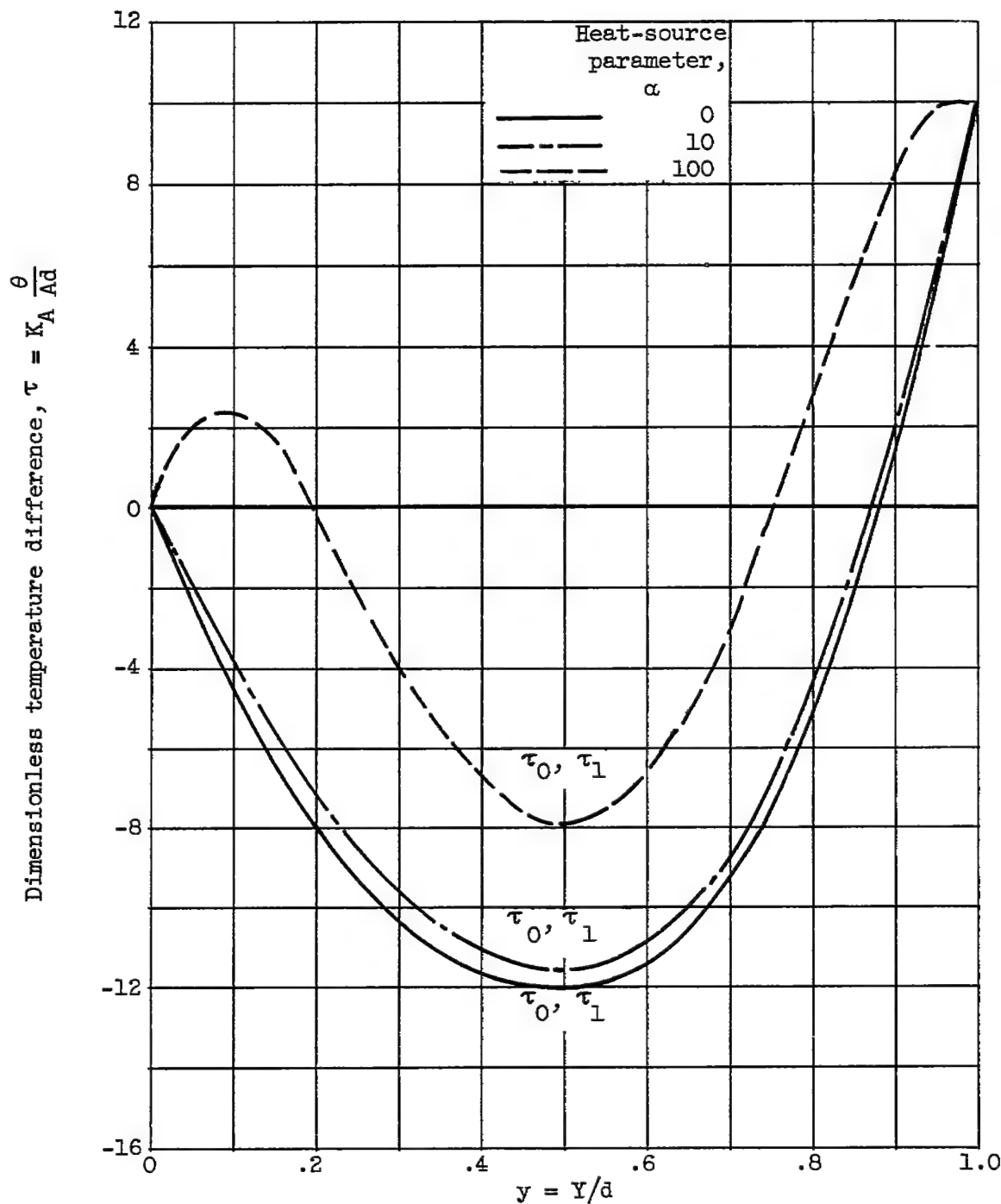
(c) $m = 2$.

Figure 8. - Concluded. Dimensionless temperature distributions for various heat-source parameters with $Ra = 1600$, $K_A = 10$, $C = -1$.

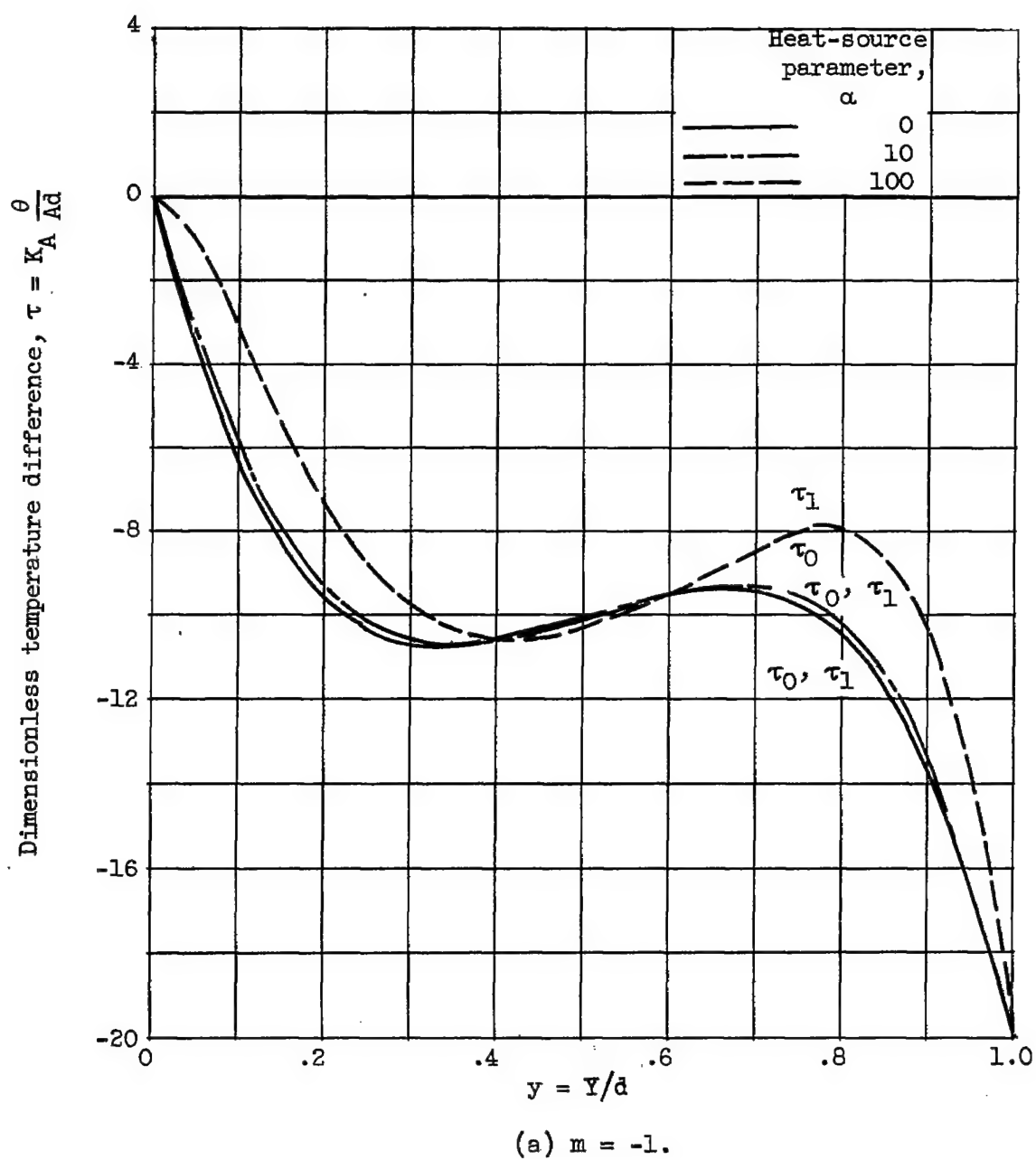


Figure 9. - Dimensionless temperature distributions for various heat-source parameters with $Ra = 10^4$, $K_A = 10$, $C = -1$.

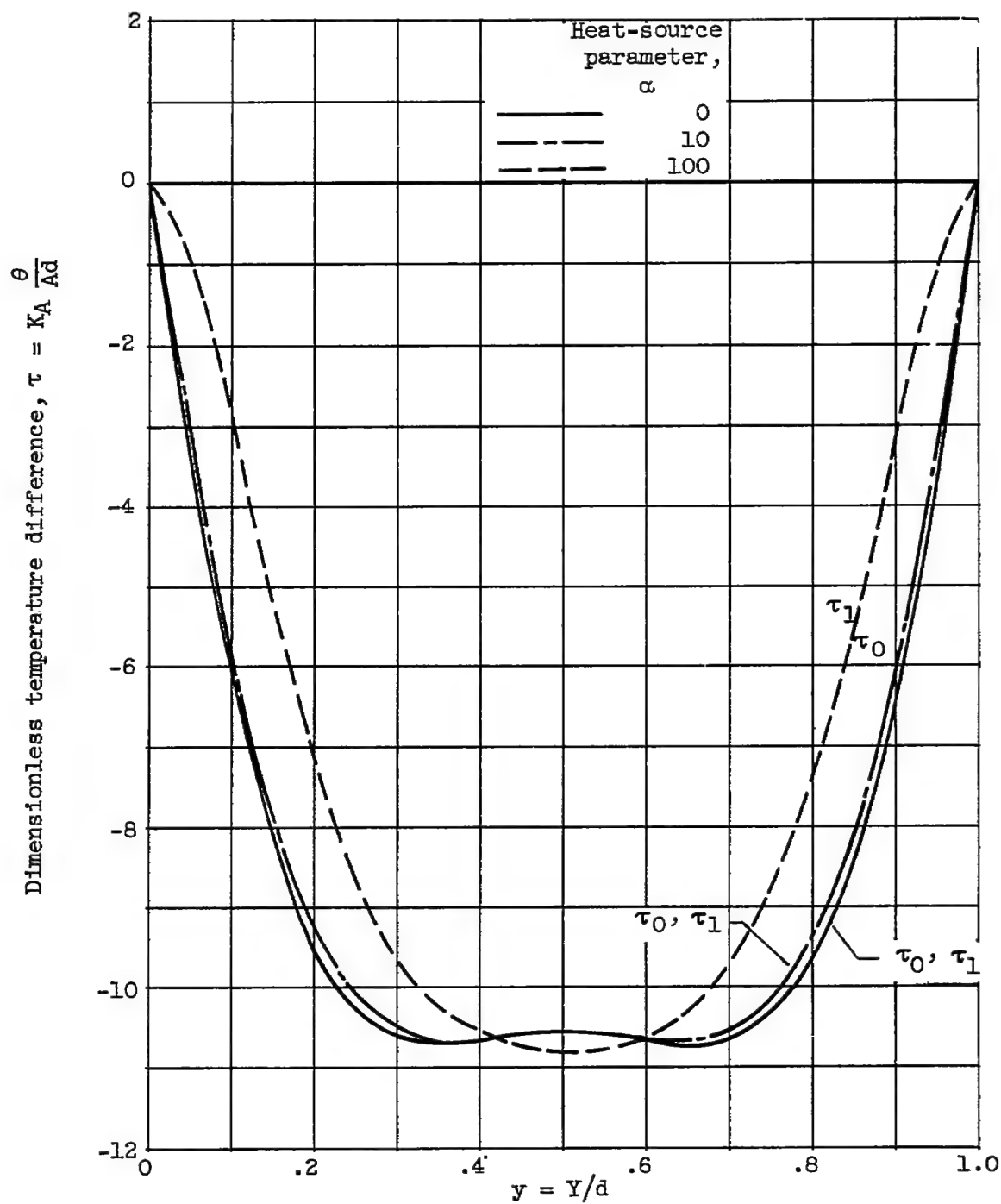
(b) $m = 1$.

Figure 9. - Continued. Dimensionless temperature distributions for various heat-source parameters with $Ra = 10^4$, $K_A = 10$, $C = -1$.

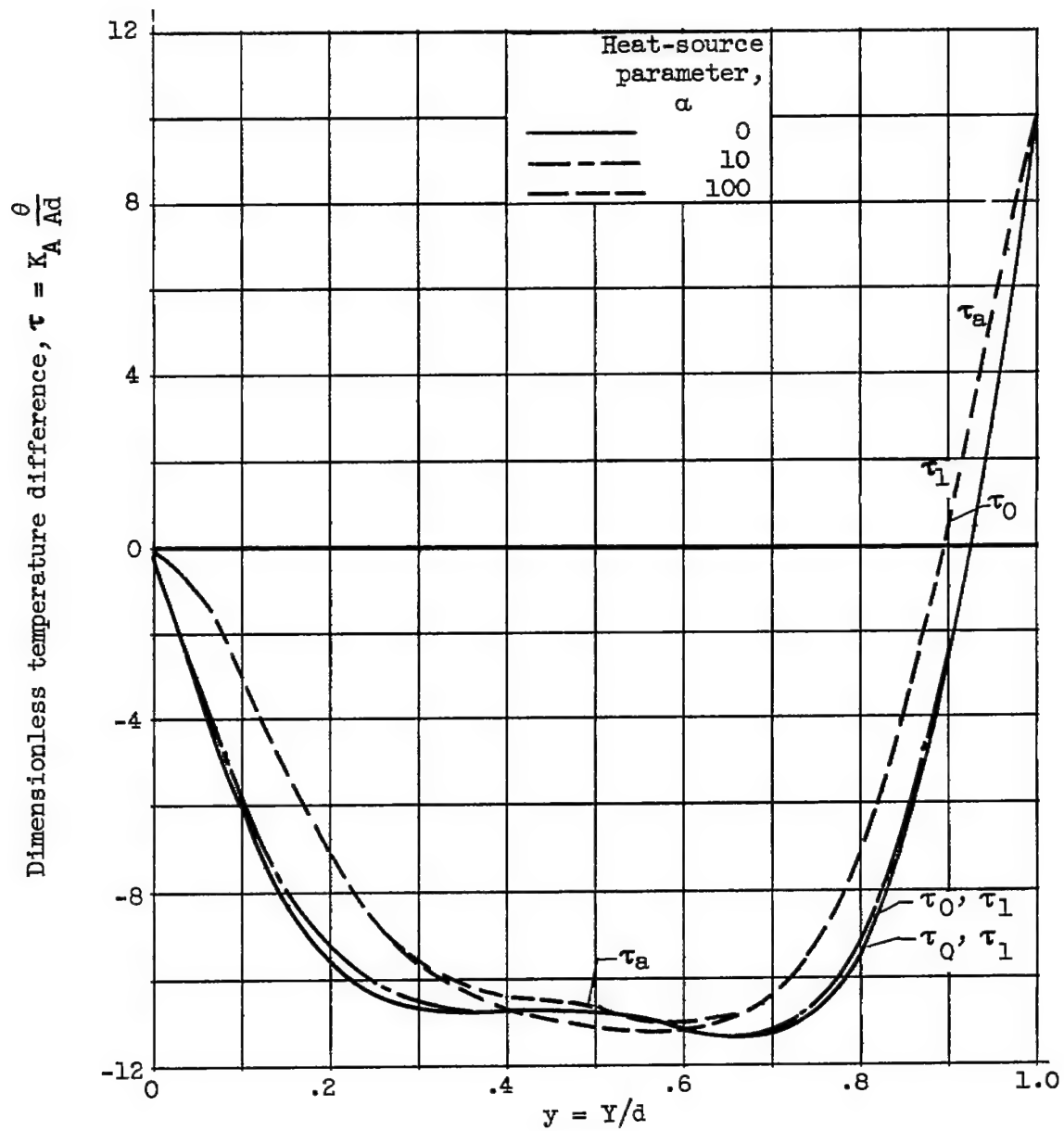
(c) $m = 2$.

Figure 9. - Concluded. Dimensionless temperature distributions for various heat-source parameters with $Ra = 10^4$, $K_A = 10$, $C = -1$.

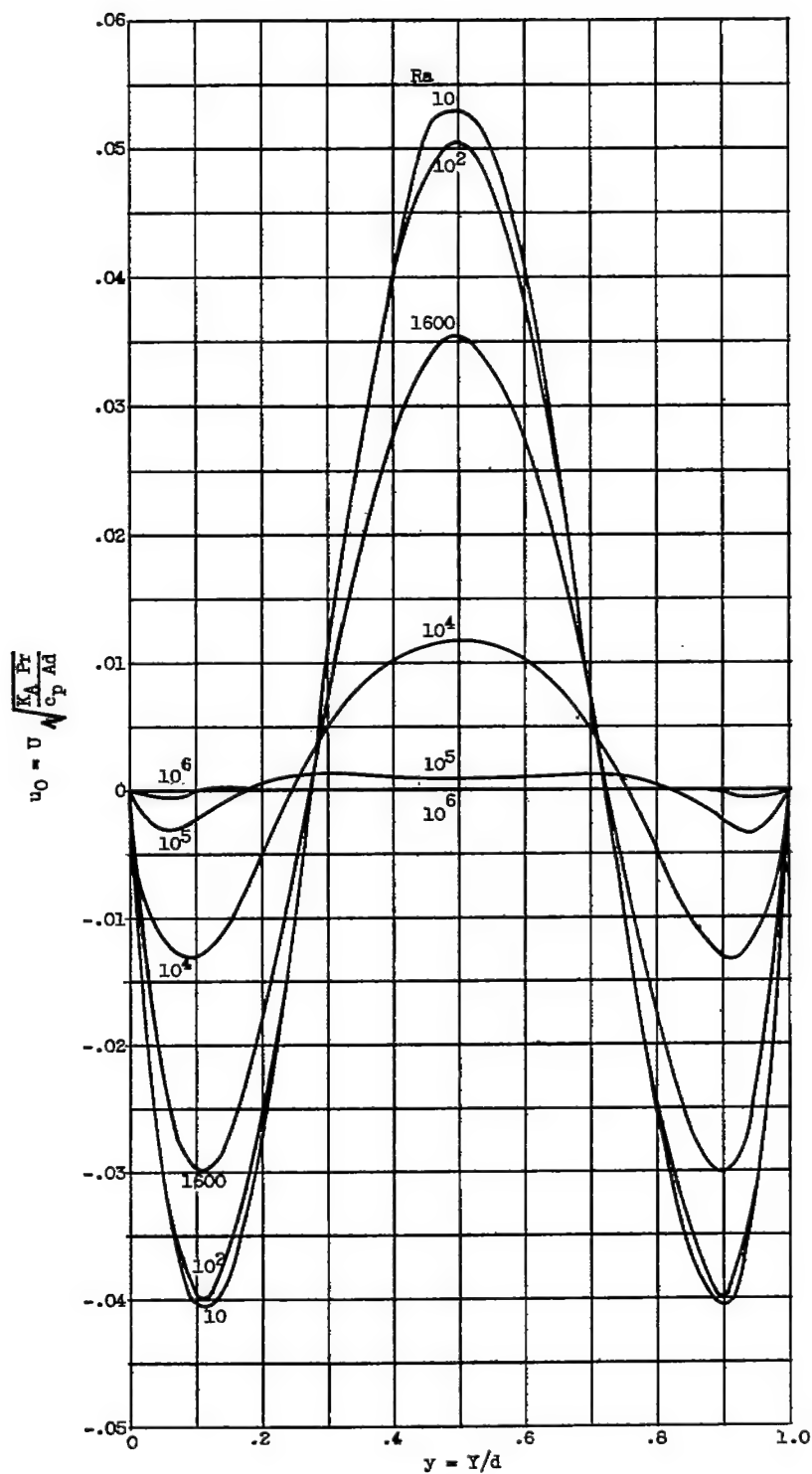


Figure 10. - Dimensionless velocities for special case of $M = 0$, $m = 1$, $K_A = 10$, and $\alpha = 10$. (Note: For $Ra = 10$, the numerical solution u coincides with given curve.)

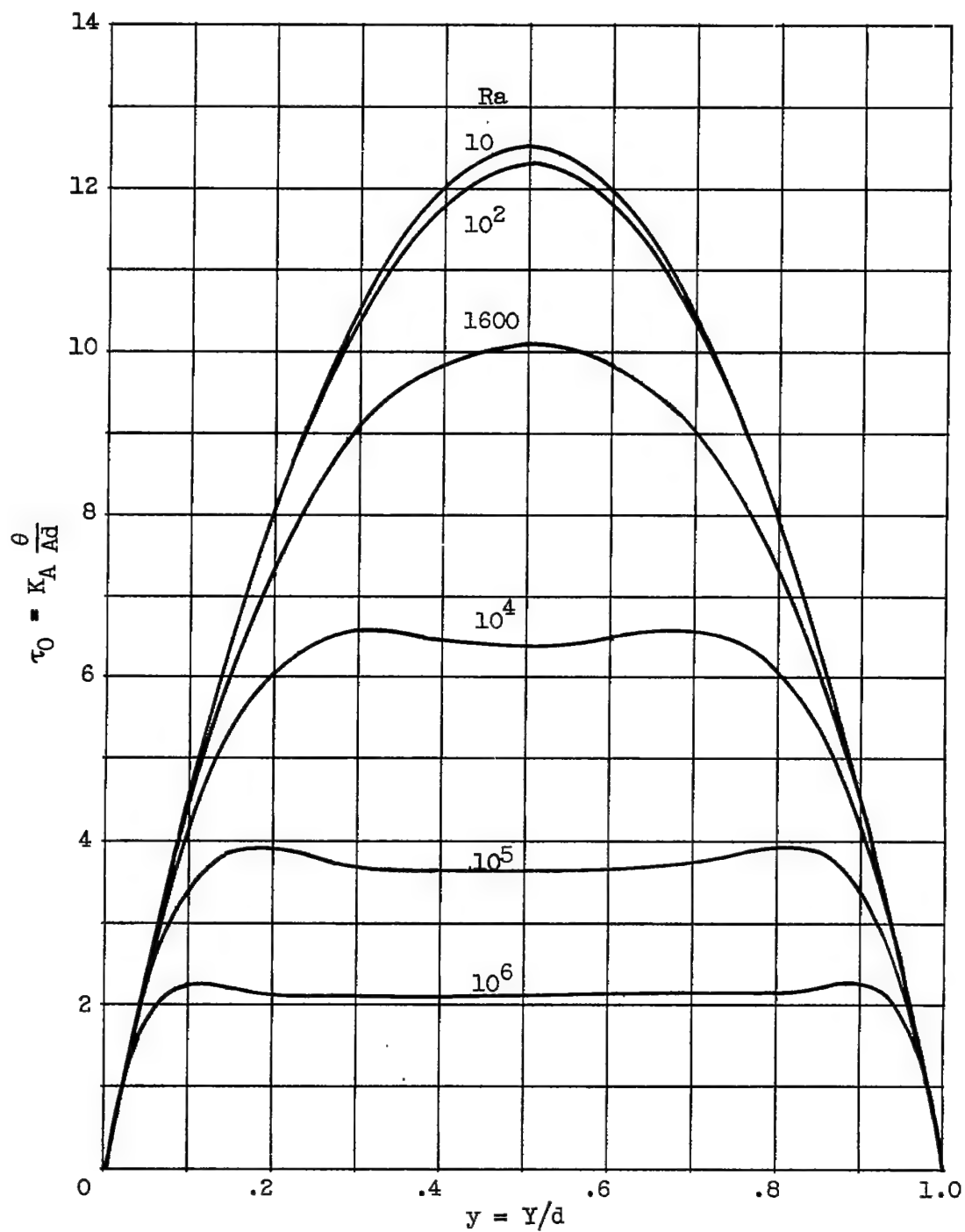


Figure 11. - Dimensionless temperatures for special case of $M = 0$, $m = 1$, $K_A = 10$, and $\alpha = 10$. (Note: For $Ra = 10$, the numerical solution τ coincides with given curve.)

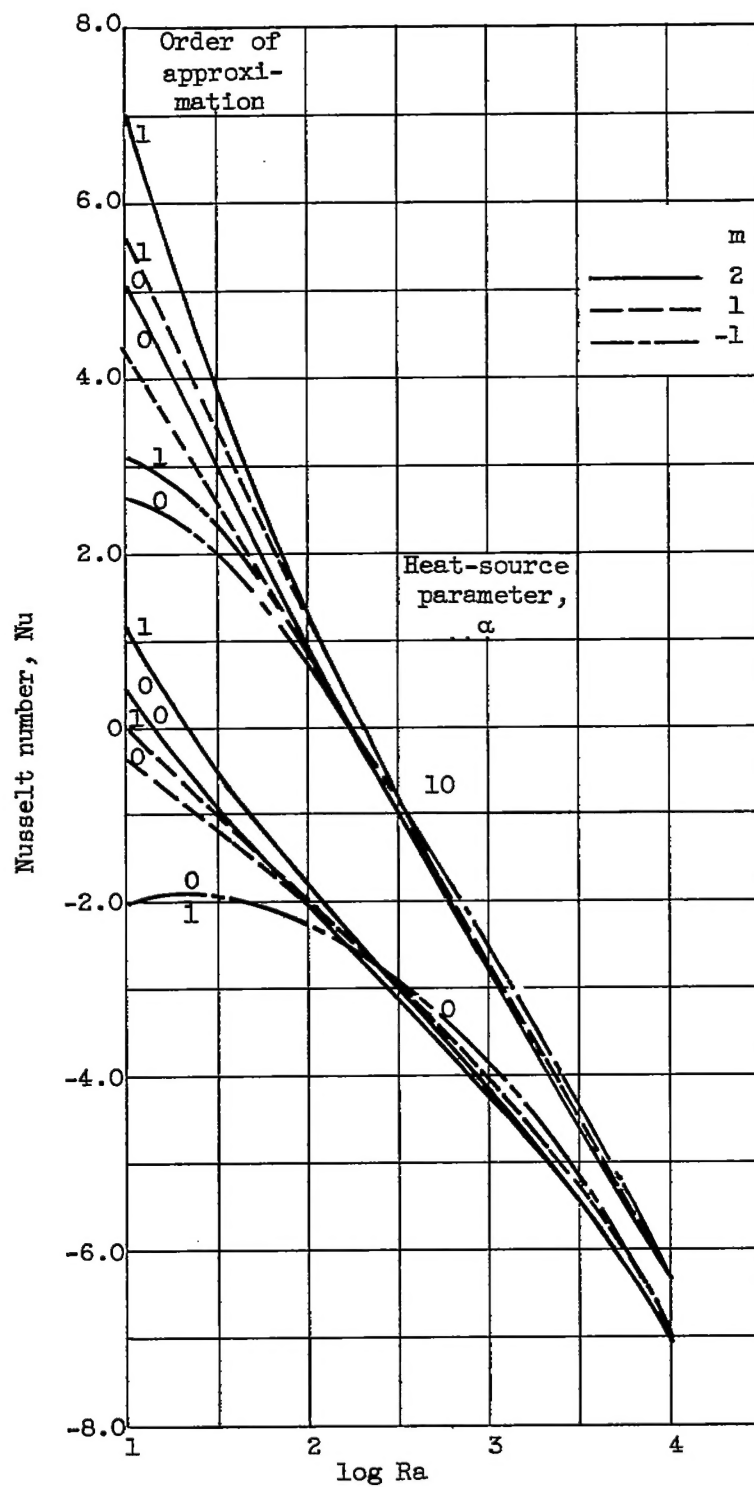


Figure 12. - Nusselt numbers for wall
at $Y = 0$ and $K_A = 10$.

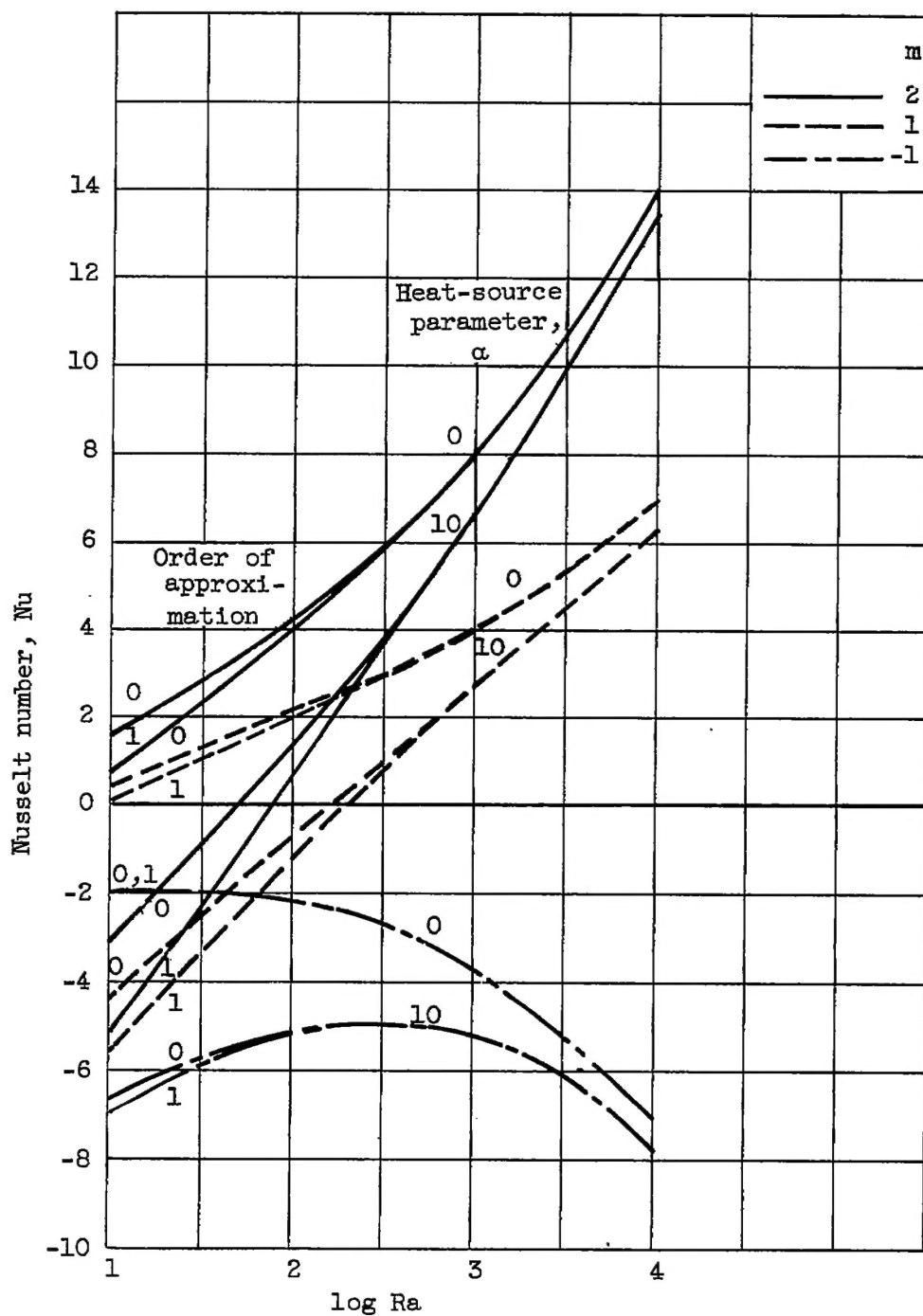


Figure 13. - Nusselt numbers for wall
at $Y = d$ and $K_A = 10$.

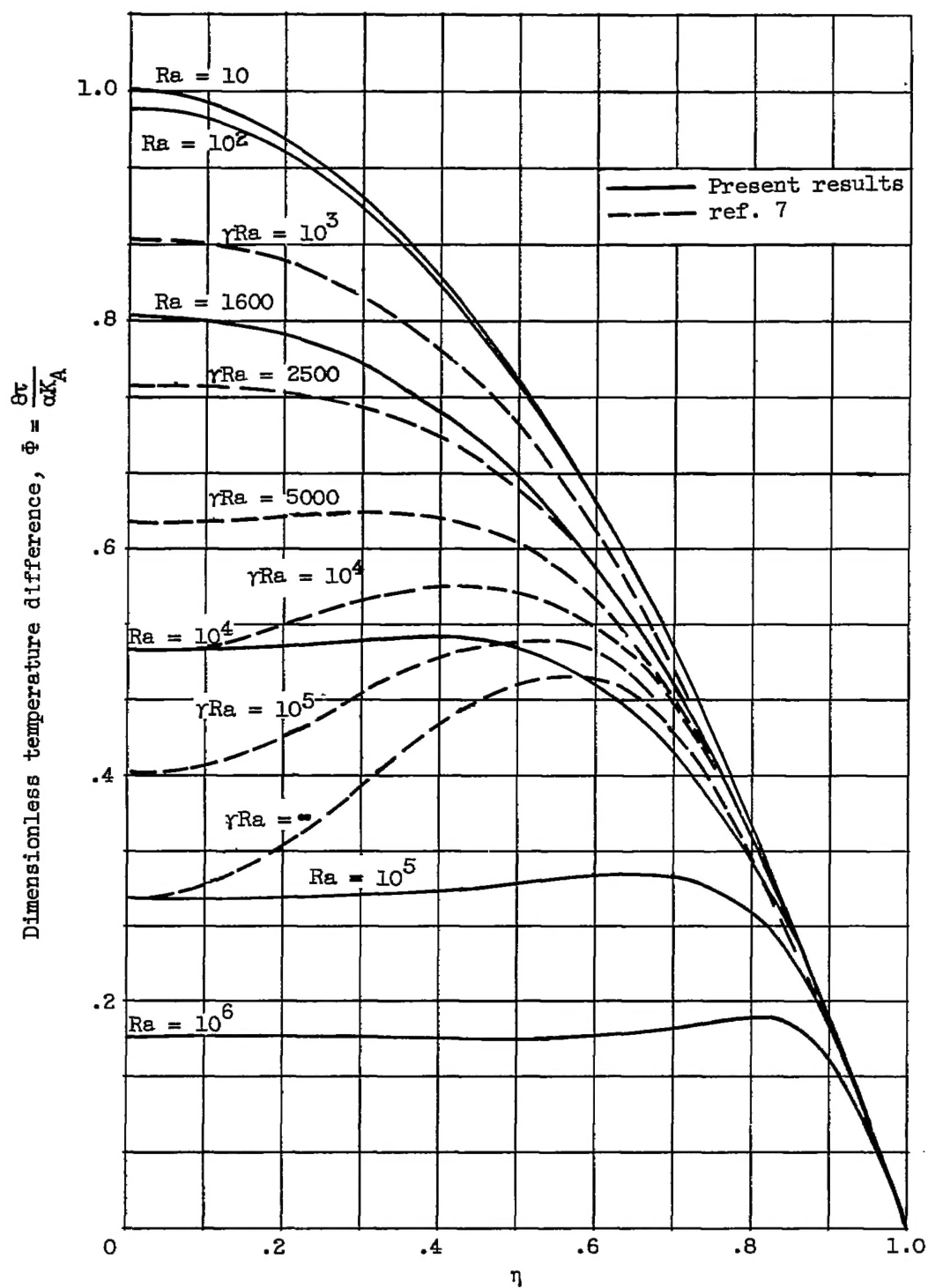


Figure 14. - Ratio of actual temperature difference to that for pure conduction for special case where $M = 0$ and $m = 1$.

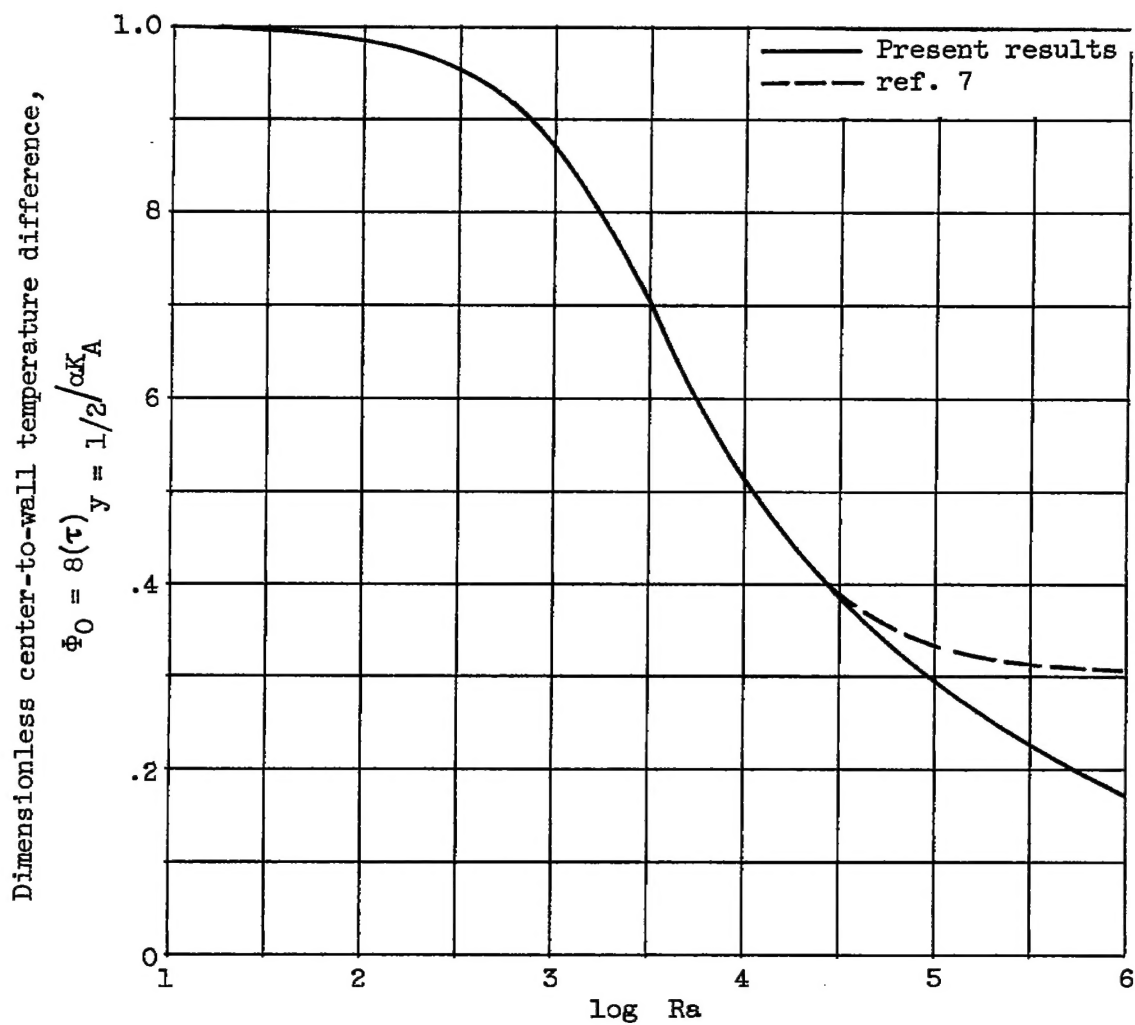


Figure 15. - Ratio of center-to-wall temperature difference to that for pure conduction for special case where $M = 0$ and $m = 1$. (Note: Dashed curve is plotted against γRa .)